Structure and Photochemistry of New Base-Stabilized Silylene (Silanediyl) Complexes $R_2(HMPA)Si{=}M(CO)_n$ of Iron, Chromium, and Tungsten (R = *t*-BuO, *t*-BuS, MesO, 1-AdaO, 2-AdaO, NeopO, TritO, Me, Cl; M = Fe, *n* = 4; M = Cr, W, *n* = 5): Sila-Wittig Reaction of the Base-Free Reactive Intermediate $[Me_2Si{=}Cr(CO)_5]$ with Dimethyl Carbonate

Christian Leis, Dallas L. Wilkinson, Hermann Handwerker, and Christian Zybill*

Anorganisch-chemisches Institut, Technische Universität München, Lichtenbergstrasse 4, W-8046 Garching, Federal Republic of Germany

Gerhard Müller

Fakultät für Chemie der Universität Konstanz, 7750 Konstanz, Federal Republic of Germany

Received August 19, 1991

The reaction of the dichlorosilanes R_2SiCl_2 (R = *t*-BuO, *t*-BuS, MesO (Mes = mesityl), 1-AdaO (Ada = adamantyl), 2-AdaO, NeopO (Neop = neopentyl), TritO (Trit = triphenylmethyl), Me, Cl) with the carbonylate dianions $M(CO)_n^{2-}$ (M = Fe, *n* = 4; M = Cr, W, *n* = 5) in the presence of HMPA (hexamethylphosphoric triamide) affords an effective access to the base-stabilized silylene complexes $R_2(HMPA)Si{=}M(CO)_n$. Single-crystal X-ray structure analyses of the iron complexes $Me_2(HMPA)Si{=}Fe(CO)_4$ (**4**) and $Cl_2(HMPA)Si{=}Fe(CO)_4$ (**5**) and the chromium compounds $Me_2(HMPA)Si{=}Cr(CO)_5$ (**7**) and $Cl_2(HMPA)Si{=}Cr(CO)_5$ (**8**) have been performed and are compared with the previously determined structures of $(t\text{-BuO})_2(HMPA)Si{=}Fe(CO)_4$ (**1**) and $(t\text{-BuO})_2(HMPA)Si{=}Cr(CO)_5$ (**6**). The structures feature relatively short M–Si bond lengths with *d*(FeSi) = 2.280 (1)/2.294 (1) (**4**) and 2.214 (1)/2.221 (1) Å (**5**) and *d*(CrSi) = 2.410 (1) (**7**) and 2.342 (1) (**8**). In contrast, the Si–O (HMPA) bonds are fairly long (1.735 (3)/1.731 (3) (**4**), 1.683 (3)/1.676 (3) (**5**), 1.743 (2) (**7**), 1.690 (2) Å (**8**)). The coordination geometry at silicon is significantly distorted from tetrahedral and subject to strong substituent effects. Both metal–silicon bond lengths and the coordination geometry at silicon in the coordination compounds correlate to frontier orbital energies and electron population densities of the free silylenes. Data from cyclic voltammetric measurements are in agreement with this description. A Mössbauer spectrum of **1** shows an unusual negative isomer shift of −0.477, which indicates particularly for the TBP d^8 compounds **1**–**5** (axial silylene coordination) a high ionic contribution of the Fe–Si bond in the sense of a betaine structure. The relative orientation of the substituents at silicon, as found in the crystal, is reproduced by a force field calculation as the global energy minimum. VT NMR experiments show the fluxionality of the ligand framework of the TBP Fe d^8 complexes at room temperature. The free energy of activation for the Berry pseudorotation process is $\Delta G_{250.0}^{\ddagger}$ = 40.3 (±5) kJ/mol. A reactivity study of the base adducts **1**, **4**, and **6** shows the photochemical activation of the silylenes: In the presence of triphenylphosphine, the trans phosphine complexes *trans*-$(t\text{-BuO})_2Si(HMPA){=}Fe(CO)_3P(C_6H_5)_3$ (**23**), *trans*-$Me_2Si(HMPA){=}Fe(CO)_3P(C_6H_5)_3$ (**24**), and *trans*-$(t\text{-BuO})_2Si(HMPA){=}Cr(CO)_4P(C_6H_5)_3$ (**26**) are obtained by a photochemical CO displacement reaction. Subsequently, the silylenes are displaced by a further phosphine molecule to yield the *trans*-bis(phosphine) complexes *trans*-$\{P(C_6H_5)_3\}_2Fe(CO)_3$ (**25**) and *trans*-$\{P(C_6H_5)_3\}_2Cr(CO)_4$ (**27**). The liberated silylenes form polysilanes; di-*tert*-butoxysilylene can be trapped in the presence of 2,3-dimethylbutadiene by an 1,4-addition to form the silacyclopentene $Si(t\text{-BuO})_2CH_2C(CH_3){=}C(CH_3)CH_2$ (**28**) (photolysis of **1**). As a secondary photolysis product, (2,3-dimethylbutadiene)iron tricarbonyl, $(\eta^4\text{-}C_6H_4)Fe(CO)_3$ (**29**), is isolated. The base-free complex $[Me_2Si{=}Cr(CO)_5]$ is generated in situ from Me_2SiCl_2 and $Na_2Cr(CO)_5$ at −50 °C as a reactive intermediate and yields a variety of interesting trapping reactions: in the presence of HMPA the stable HMPA adduct **7** is formed; the thermolabile THF adduct $Me_2Si(THF){=}Cr(CO)_5$ (**32**) dimerizes above −40 °C to give **21**. With dimethyl carbonate as the trapping reagent, $[Me_2Si{=}Cr(CO)_5]$ undergoes a sila-Wittig reaction to form hexamethyltrisiloxane, $[Me_2SiO{-}]_3$ (**30**), and (dimethoxycarbene)chromium pentacarbonyl, $(MeO)_2C{=}Cr(CO)_5$ (**31**).

Introduction

Currently, the organometallic chemistry of silicon[1-5] is in a remarkable period of renaissance. An increasing number of publications, particularly in the area of coordination chemistry with low-valent silicon ligands, indicates this development.[6,7] Extensive research activities have led to the synthesis of a variety of a new organometallic silicon compounds such as silylene (silanediyl) complexes A[8] and B[9-13] (with a base at silicon), cationic

(1) Speier, J. L. *Adv. Organomet. Chem.* **1977**, *17*, 407.
(2) Mackay, K. M.; Nicholson, B. K. In *Comprehensive Organometallic Chemistry*; Wilkinson, G., Stone, F. G. A., Abel, E. W., Eds.; Pergamon Press: Oxford, U.K., 1982.
(3) Aylett, B. J. *Adv. Inorg. Chem. Radiochem.* **1982**, *25*, 1.
(4) Curtis, M. D.; Epstein, P. S. *Adv. Organomet. Chem.* **1981**, *19*, 213.
(5) Aylett, B. J. *J. Organomet. Chem. Libr.* **1980**, *9*, 327.
(6) Zybill, C. *Top. Curr. Chem.* **1991**, *160*, 1.
(7) Tilley, T. D. In *The Chemistry of Organosilicon Compounds*; Patai, S., Rappoport, Z., Eds.; Wiley: New York, 1989.
(8) (a) Straus, D. A.; Grumbine, S. D.; Tilley, T. D. *J. Am. Chem. Soc.* **1990**, *112*, 7801. (b) Leis, C.; Handwerker, H.; Wilkinson, D. L.; Müller, G.; Zybill, C. IXth International Symposium on Organosilicon Chemistry, Edinburgh, Scotland, July 16–20, 1990, Abstract C6.
(9) Zybill, C.; Müller, G. *Angew. Chem.* **1987**, *99*, 639; *Angew. Chem., Int. Ed. Engl.* **1987**, *26*, 669.

0276-7333/92/2311-0514$03.00/0

Chart I

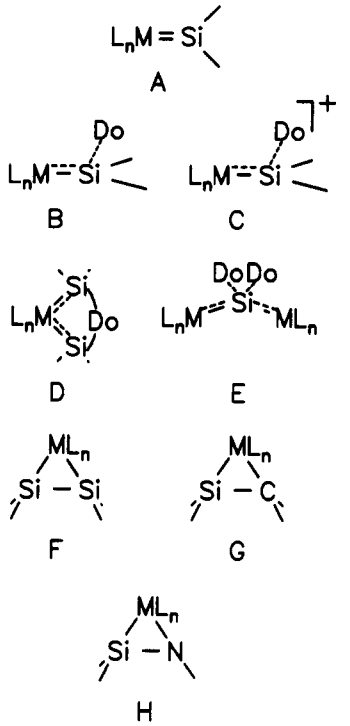

silylene complexes C,[14] cyclic bis(silylene) complexes D,[15-17] and base adducts of metallasilaallenes E,[18] as well as disilene (F),[19-21] silene (G),[22,23] and silaimine (H)[23] complexes (Chart I). This development has gained considerable impetus from the discovery of stable coordination compounds of silylenes (silanediyls), either as neutral (B)[6-13] or as cationic base adducts (C).[14]

Much evidence can be found in the literature for silylene complexes as reactive intermediates, e.g. in catalytic silylene transfer reactions to olefins and acetylenes[24] or in dehydrogenative coupling reactions of silanes with late transition metals.[25,26] Nevertheless, stable compounds have only been obtained recently. Indications for the thermodynamic stability of base adducts B have been provided the first time by Schmid with the complexes $(CO)_4Fe{=}Si(HNEt_2)Me_2$ and $(OC)_4Fe{=}Si(Cl)NPhCH_2CH_2NHPh$. Both compounds decompose above −20 °C and have been characterized by NMR, IR, and mass spectroscopy.[27] Stable base adducts of silylene complexes were finally be synthesized in 1987 in our department with the compound $(t\text{-BuO})_2(HMPA)Si{=}Fe(CO)_4$[9] and by Tilley with the cationic complex $[Cp^*(Me_3P)_2Ru{=}Si(MeCN)Ph_2^+]BPh_4^-$.[14] In the meantime further examples have become known and have in most instances also been characterized by single-crystal X-ray structure analysis. Nevertheless, the compounds reported so far in the literature are still singular cases and their chemistry remains virtually unexplored. Therefore, a systematic investigation of this class of compounds as well as their chemistry appeared to be necessary.

Table I. ^{29}Si NMR Data for Selected Silylene Complexes

compd	δ/ppm	$^2J(^{31}P^{29}Si)$/Hz
$(OC)_4FeSi(HMPA)(t\text{-BuO})_2$ (1)	7.1	26.4
$(OC)_4FeSi(HMPA)(t\text{-BuS})_2$ (3)	74.7	25.3
$(OC)_4FeSi(HMPA)Me_2$ (4)	92.3	17.5
$(OC)_4FeSi(HMPA)Cl_2$ (5)	59.7	31.2
$(OC)_5CrSi(HMPA)(t\text{-BuO})_2$ (6)	12.7	37.2
$(OC)_5CrSi(HMPA)Me_2$ (7)	101.4	31.3
$(OC)_5CrSi(HMPA)Cl_2$ (8)	55.0	41.4
$(OC)_5CrSi(HMPA)(1\text{-AdaO})_2$ (9)	11.9	30.1
$(OC)_5CrSi(HMPA)(2\text{-AdaO})_2$ (10)	11.7	30.2
$(OC)_5CrSi(HMPA)(NeopO)_2$ (11)	12.5	31.1
$(OC)_5CrSi(HMPA)(TritO)_2$ (12)	10.9	32.0
$(OC)_5CrSi(HMPA)(t\text{-BuS})_2$ (14)	83.2	31.0
$[Cp^*(Me_3P)_2RuSi(MeCN)Ph_2]^+BPh_4^-$ (17)	95.8[14b]	
$Cp^*(Me_3P)_2RuSi(OTf)Ph_2$ (18)	112.4[14b]	
$(OC)_4FeSi(t\text{-BuS})_2$ (19)	75.7	
$(OC)_4Fe{=}Si(HMPA)_2{=}Fe(CO)_4$ (20)	24.1	22.0

In this paper, a comparative study of the structure and reactivity of a series of base-stabilized silylene complexes is presented with the focus on electronic and steric effects that influence the coordination of silylene ligands to transition metals. Furthermore, some exemplary silylene transfer and trapping reactions are reported. A preliminary report of 4 has appeared;[12] the structures of 1, 3, and 6 have already been discussed in detail.[10]

Synthesis

A wide arsenal of synthetic methods is available for the formation of metal–silicon bonds, but only a few allow a general and effective access to silylene complexes. Reactions of dichlorosilanes with metalate anions are, however, quite general and can be employed to prepare base-stabilized silylene complexes of various (Fe, Ru, Os, Cr, W, Re) metals (eqs 1 and 2). The method allows the use of both mono- and dinuclear metalate anions (eq 3).

(10) Zybill, C.; Müller, G. *Organometallics* **1988**, *7*, 1368.
(11) Zybill, C. *Nachr. Chem., Tech. Lab.* **1989**, *37*, 248.
(12) Zybill, C.; Wilkinson, D. L.; Leis, C.; Müller, G. *Angew. Chem.* **1989**, *101*, 206; *Angew. Chem., Int. Ed. Engl.* **1989**, *28*, 203.
(13) Jutzi, Z.; Möhrke, A. *Angew. Chem., Int. Ed. Engl.* **1990**, *29*, 893.
(14) (a) Straus, D. A.; Tilley, T. D.; Rheingold, A. L.; Geib, S.; *J. Am. Chem. Soc.* **1987**, *109*, 5872. (b) Straus, D. A.; Zhang, C.; Quimbita, G.; Grumbine, S. D.; Heyn, R. H.; Tilley, T. D.; Rheingold, A. L.; Geib, S. J. *J. Am. Chem. Soc.* **1990**, *112*, 2673.
(15) Malisch, W.; Lorz, P.; Thum, G. *Chemiedozententagung*; 1988, *abs. B 36*, 13.-16.3., Mainz, FRG.
(16) Ueno, K.; Tobita, H.; Shimoi, M.; Ogino, H. *J. Am. Chem. Soc.* **1988**, *110*, 4092.
(17) Tobita, H.; Ueno, K.; Shimoi, M.; Ogino, H. *J. Am. Chem. Soc.* **1990**, *112*, 3415–3420.
(18) Zybill, C.; Wilkinson, D. L.; Müller, G. *Angew. Chem.* **1988**, *100*, 574; *Angew. Chem., Int. Ed. Engl.* **1988**, *27*, 583.
(19) Pham, E. K.; West, R. 20th Organosilicon Symposium; Tarrytown, NY, April 18–19, 1986; Abstract P 23.
(20) Pham, E. K.; West, R. *J. Am. Chem. Soc.* **1989**, *111*, 7667.
(21) Berry, D. H.; Chey, J.; Zipin, H. S.; Carroll, P. J. *J. Am. Chem. Soc.* **1990**, *112*, 452.
(22) Campion, B. K.; Heyn, R. H.; Tilley, T. D. *J. Am. Chem. Soc.* **1988**, *110*, 7558.
(23) Berry, D. H. IXth International Symposium on Organosilicon Chemistry; Edinburgh, Scotland, July 16–20, 1990; Abstract C12.
(24) (a) Ojima, I.; Inaba, S. I.; Kogure, T.; Nagai, Y. *J. Organomet. Chem.* **1973**, *55*, C7. (b) Yamamoto, K.; Okinoshima, H.; Kumada, M. *J. Organomet. Chem.* **1971**, *27*, C31. (c) Kumada, M. *J. Organomet. Chem.* **1975**, *100*, 127. (d) Seyferth, D.; Shannon, M. L.; Vick, S. C.; Lim, T. F. O. *Organometallics* **1985**, *4*, 57. (e) Okinoshima, H.; Yamamoto, K.; Kumada, M. *J. Am. Chem. Soc.* **1972**, *94*, 9263. (f) Sukurai, H.; Kamiyama, Y.; Nakadaira, Y. *J. Am. Chem. Soc.* **1977**, *99*, 3879. (g) Pannell, K. H.; Cervantes, J.; Hernandez, C.; Cassias, J.; Vincenti, S. *Organometallics* **1986**, *5*, 1056. (h) Tobita, H.; Ueno, K.; Ogino, H. *Chem. Lett.* **1986**, 1777. (i) Tobita, H.; Ueno, K.; Ogino, H. *Bull. Chem. Soc. Jpn.* **1988**, *61*, 2797. (j) Thum, G.; Malisch, W. *J. Organomet. Chem.* **1984**, *264*, C5. (k) Kang, H.; Jacobson, D. B.; Shin, S. K.; Beauchamp, J. L.; Bowere, M. T. *J. Am. Chem. Soc.* **1986**, *108*, 5668.
(25) Brown-Wensley, K. *Organometallics* **1987**, *6*, 1590.
(26) (a) Harrod, J. F. *Polyhedron* **1991**, *10*, 1239. (b) Chang, L. S.; Corey, J. Y. *Organometallics* **1989**, *8*, 1885. (c) Corey, J. Y.; Chang, L. S.; Corey, E. R. *Organometallics* **1987**, *6*, 1595.
(27) Schmid, G.; Welz, E. *Angew. Chem.* **1977**, *89*, 823; *Angew. Chem., Int. Ed. Engl.* **1977**, *16*, 785.
(28) Leis, C.; Handwerker, H.; Wilkinson, D. L.; Müller, G.; Zybill, C. EICS II; Wiesbaden, FRG, april 16–20, 1990; P 4.

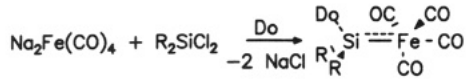

R = t-BuO 1
R = MesO 2
R = t-BuS 3
R = CH_3 4
R = Cl 5

(1)

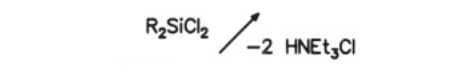

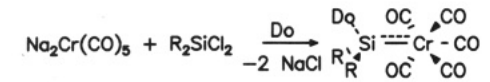

Do = HMPA

R = t-BuO 6
R = CH_3 7
R = Cl 8
R = 1-AdaO 9
R = 2-AdaO 10
R = NeopO 11
R = TritO 12

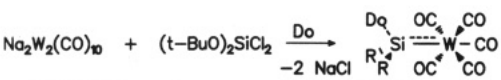

Do = HMPA $-W(CO)_5Do$ 13

The reaction of dichlorosilanes with $Na_2Fe(CO)_4$ (eq 4) is a nucleophilic displacement at silicon followed by NaCl elimination. The reaction kinetic is too fast for an in-

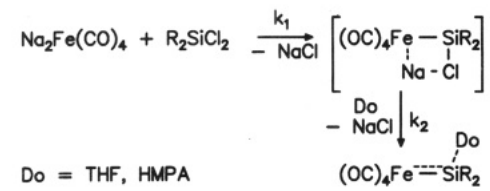

Do = THF, HMPA

(4)

vestigation by NMR techniques; however, it can be assumed that $k_2 \geq k_1$, since no intermediates have been detected. In the presence of HMPA, $Na_2Fe(CO)_4$ forms the ion pair $Na^+[Na^+(HMPA)Fe(CO)_4^{2-}]$,[29] which can be isolated in the form of dark red crystals. The presence of HMPA is essential for providing ion solvation and tuning the redox potential of the $Fe(CO)_4^{2-}$ ion. In most cases, the use of only stoichiometric amounts of HMPA has proven to be sufficient.

Whereas HMPA adducts of silylene complexes can be prepared in high yields, adducts of other donor solvents such as THF (tetrahydrofuran) or DME (1,2-dimethoxyethane) are much less stable and can only be detected at low temperatures by NMR spectroscopy. These thermolabile compounds dimerize at higher temperatures.

NMR Spectroscopy

The silylene complexes prepared (eqs 1–3) were characterized by ^1H, ^{29}Si, and ^{13}C NMR spectroscopy (Tables I and II). The ^1H NMR spectra of the complexes display a characteristic shift pattern and allow an unambiguous structure assignment; for instance, HMPA shows a typical upfield shift of the CH_3 signals upon coordination to the silicon.

Temperature-dependent NMR spectra provide further information about the molecular dynamics. According to VT ^1H-NMR experiments, rotation around the metal–silicon bond is restricted only by steric requirements of the ligands. A similar observation has been made, e.g., for trigonal bipyramidal d^8 Co complexes $X_3SiCo(CO)_4$ (X = F, Cl, Br, H, Ph).[30]

Table II. IR Data for Silylene Complexes

compd	ν_{CO}/cm^{-1}	$k/N\ m^{-1}$
$(OC)_4FeSi(HMPA)(t\text{-}BuO)_2$ (1)	2005, 1920, 1883	1623, 1489, 1432
$(OC)_4FeSi(HMPA)(NEt_2)_2$ (15)	1998, 1926, 1888	1612, 1498, 1439
$(OC)_4RuSi(HMPA)(t\text{-}BuO)_2$ (16)	2022, 1946, 1898	1651, 1529, 1455
$(OC)_5CrSi(HMPA)(t\text{-}BuO)_2$ (6)	2015, 1991, 1930	1640, 1601, 1504
$(OC)_5CrSi(HMPA)Me_2$ (7)	2100, 2075, 1975	1781, 1739, 1575

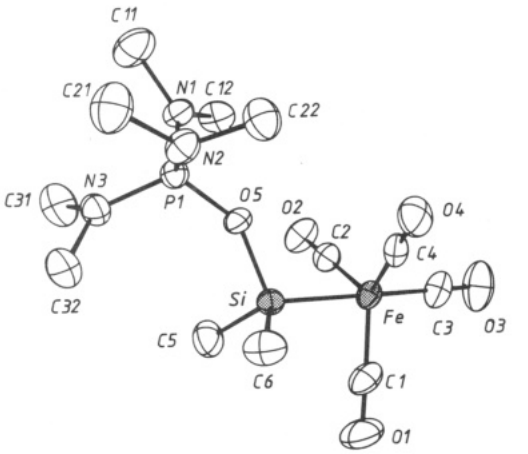

Figure 1. Molecular structure of one of the crystallographically independent molecules of $(CO)_4Fe{=}Si(HMPA)Me_2$ (4) and the crystal numbering scheme used (ORTEP, displacement ellipsoids at the 50% probability level; hydrogen atoms omitted for clarity).

The ^{29}Si-NMR[31] chemical shifts of base-stabilized silylene complexes fall in a characteristic range between 0 and 140 ppm, which allows a clear distinction of silylene complexes from various silylmetal compounds and also, e.g., from dimeric 1,3-disilacyclobutanes, which are typically observed at rather low field below 150 ppm.

However, no linear correlation between the electronegativity of the particular substituents at silicon and observed ^{29}Si NMR shifts can be measured (Tables I and II). Rather, a square dependency between the overall electronegativity of the substituents and the ^{29}Si-NMR shifts is found which is in accordance with the assumption of a superposition of diamagnetic and paramagnetic shift influences on silicon.[32] The observed gradation (O-*t*-Bu, S-*t*-Bu, Me, Cl) of ^{29}Si resonances of the compounds is analogous to the shifts known for regular tetravalent silicon compounds. Furthermore, the shift differences for $R_2(HMPA)Si{=}ML_n$ vs R_2SiCl_2 are also diagnostic. The ^{29}Si-NMR signals for compounds with homologous metals show a typical upfield shift for the heavier metal.

The coupling constant $J = (^{31}P^{29}Si)$ between HMPA and Si is practically invariant over a temperature range from

(29) Colman, J. P.; Finke, R. G.; Cawse, J. N.; Brauman, J. I. *J. Am. Chem. Soc.* **1977**, *99*, 2515.

(30) (a) Lichtenberger, D. L.; Brown, T. L. *J. Am. Chem. Soc.* **1977**, *99*, 8187–8194. (b) Vancea, L.; Pomeroy, R. K.; Graham, W. A. G. *J. Am. Chem. Soc.* **1976**, *98*, 1407–1413. (c) Krentz, R.; Pomeroy, R. K. *Inorg. Chem.* **1985**, *24*, 2976–2980.

(31) The ^{29}Si NMR spectra of silylene complexes and their various donor adducts have in most cases been acquired by conventional techniques with small pulse angles to cut down pulse delay times. (The T_1 relaxation times of silicon species can be extraordinarily high; for instance, T_1 = 100 s for $(Me_2SiO)_4$). In cases where a $J(^1H^{29}Si)$ coupling was available for polarization transfer, pulse sequence methods such as INEPT or DEPT have been applied with the parameters $^2J(^1H^{29}Si)$ = 7.2 Hz, n = 3, $\gamma = 1/4J$ = 34.7 ms; $\Delta_{opt} = (1/nJ)$ arcsin $n^{-1/2}$ = 27.2 ms for a $Si(CH_3)_2$ unit (INEPT). Cf. also: Blinka, T. A.; Bradley, J. H.; West, R. *Adv. Organomet. Chem.* **1984**, *23*, 193.

(32) Ernst, C. R.; Spialter, L.; Buell, G. R.; Wilhite, D. L. *J. Am. Chem. Soc.* **1974**, *96*, 5375–5381.

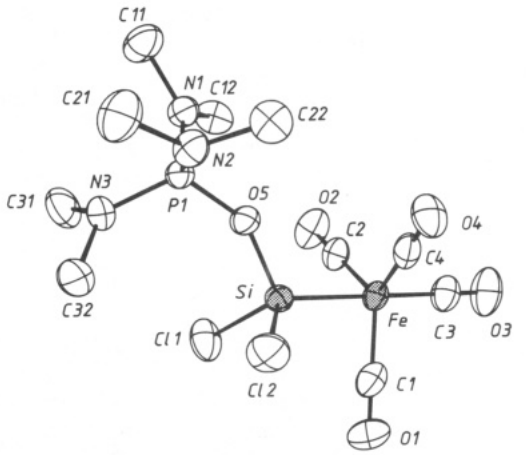

Figure 2. Molecular structure of one of the crystallographically independent molecules of $(OC)_5Fe{=}Si(HMPA)Cl_2$ (**5**) in the crystal.

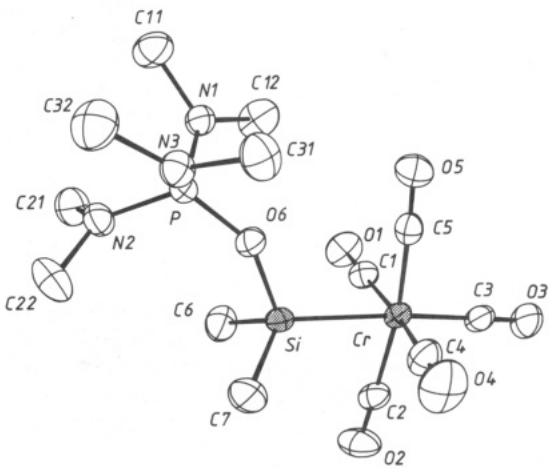

Figure 3. Molecular structure of $(CO)_5Cr{=}Si(HMPA)Me_2$ (**7**) in the crystal.

−90 to +110 °C due to a rigid coordination of the HMPA molecule to silicon. Only in the case of the methyl compound **4** is a slight line broadening of the HMPA signal observed above 25 °C, which is indicative of the beginning of an exchange process between **4** and a HMPA-free complex.

The ^{13}C-NMR data for the silylene complexes (with a base at silicon), and in particular the resonances of the coordinated metal carbonyls, are similar to data for analogous carbene complexes. A variable-temperature NMR investigation of $(t\text{-BuO})_2(HMPA)Si{=}Fe(CO)_4$ (**1**) shows the fluxionality of the coordination polyhedron at the metal. For $Me_2(HMPA)Si{=}Fe(CO)_4$ (**4**) the free energy of activation for this process has been measured as $\Delta G^{\ddagger} = 40.3\ (\pm 5)$ kJ/mol (9.63 kcal/mol, $T_c = -80.0$ °C).

For comparison, similar trigonal bipyramidal cobalt compounds $R_3SiCo(CO)_4$ have free energies of activation for the Berry pseudorotation process: $\Delta G^{\ddagger} = 6.9$ kcal/mol ($T_c = -114$ °C), R = F; $\Delta G^{\ddagger} = 8.3$ kcal/mol ($T_c = -85$ °C), R = Cl; $\Delta G^{\ddagger} = 9.5$ kcal/mol ($T_c = -61$ (4) °C), R = Ph.[30]

Solid-State Structures

In order to gain further insight into the nature of the silylene–metal bonding and the role of the complexing HMPA donor molecules, the single-crystal X-ray structures of **4**, **5**, **7**, and **8** were determined (Tables III–X; Figures 1–4). Together with the previously determined structures of **1**, **3**, and **6** they allow a detailed discussion of the role

Table III. Selected Interatomic Distances (Å) and Angles (deg) in the Crystal Structures of 4 and 5[a]

	4[b]	5[b]
	Bond Distances	
Fe–Si	2.280 (1)/2.294 (1)	2.214 (1)/2.221 (1)
Fe–C3	1.792 (6)/1.783 (5)	1.793 (5)/1.796 (5)
Fe–C1	1.764 (6)/1.754 (5)	1.775 (6)/1.769 (5)
Fe–C2	1.756 (5)/1.755 (6)	1.779 (5)/1.769 (5)
Fe–C4	1.758 (5)/1.753 (5)	1.778 (5)/1.780 (5)
Si–O5	1.735 (3)/1.731 (3)	1.683 (3)/1.676 (3)
Si–C5 (Si–Cl1)[c]	1.862 (5)/1.855 (5)	2.082 (1)/2.079 (2)
Si–C6 (Si–Cl2)[c]	1.866 (5)/1.858 (5)	2.080 (2)/2.081 (2)
P–O5	1.528 (3)/1.520 (3)	1.552 (3)/1.548 (3)
C3–O3	1.137 (6)/1.147 (5)	1.143 (5)/1.127 (5)
C1–O1	1.155 (5)/1.167 (5)	1.149 (6)/1.153 (5)
C2–O2	1.160 (5)/1.156 (5)	1.146 (5)/1.155 (5)
C4–O4	1.161 (5)/1.163 (5)	1.150 (5)/1.144 (5)
P–N1	1.607 (4)/1.614 (4)	1.605 (3)/1.602 (4)
P–N2	1.629 (4)/1.613 (4)	1.613 (3)/1.611 (3)
P–N3	1.613 (4)/1.624 (4)	1.613 (3)/1.614 (4)
N1–C11	1.458 (6)/1.464 (6)	1.460 (6)/1.459 (6)
N1–C12	1.448 (6)/1.453 (6)	1.468 (5)/1.480 (6)
N2–C21	1.463 (6)/1.476 (6)	1.479 (5)/1.468 (6)
N2–C22	1.468 (5)/1.457 (6)	1.460 (5)/1.443 (6)
N3–C31	1.457 (6)/1.425 (7)	1.461 (6)/1.421 (7)
N3–C32	1.463 (6)/1.459 (6)	1.473 (6)/1.470 (6)
	Bond Angles	
Fe–Si–C5 (Fe–Si–Cl1)[c]	115.5 (2)/116.8 (2)	117.5 (1)/118.9 (1)
Fe–Si–C6 (Fe–Si–Cl2)[c]	115.6 (2)/115.2 (2)	116.7 (1)/117.2 (1)
C5–Si–C6 (Cl1–Si–Cl2)[c]	107.9 (2)/107.8 (2)	102.1 (1)/101.6 (1)
Fe–Si–O5	110.4 (1)/109.6 (1)	114.5 (1)/113.2 (1)
C5–Si–O5 (Cl1–Si–O5)[c]	102.3 (2)/101.8 (2)	101.2 (1)/100.7 (1)
C6–Si–O5 (Cl2–Si–O5)[c]	103.6 (2)/104.1 (2)	102.3 (1)/102.7 (1)
Si–O5–P	146.3 (2)/148.4 (2)	147.1 (2)/148.2 (2)
O5–P–N1	104.7 (2)/117.3 (2)	103.7 (2)/117.2 (2)
O5–P–N2	107.6 (2)/106.9 (2)	106.7 (2)/105.7 (2)
O5–P–N3	116.1 (2)/103.7 (2)	115.6 (2)/102.9 (2)
Si–Fe–C3	178.9 (2)/177.5 (2)	179.4 (2)/177.5 (1)
Si–Fe–C1	83.0 (2)/83.4 (2)	85.0 (2)/86.2 (1)
Si–Fe–C2	84.4 (1)/83.4 (1)	85.1 (1)/85.2 (1)
Si–Fe–C4	83.0 (1)/84.7 (2)	84.8 (1)/86.1 (1)
Fe–C3–O3	179.2 (5)/177.8 (5)	179.0 (4)/178.9 (4)
Fe–C1–O1	178.5 (5)/178.4 (4)	179.5 (4)/179.4 (4)
Fe–C2–O2	179.2 (4)/178.8 (4)	179.2 (4)/179.0 (4)
Fe–C4–O4	179.1 (4)/178.8 (4)	178.0 (4)/179.4 (4)

[a] Estimated standard deviations in units of the last significant figure are given in parentheses. [b] Both values for the two crystallographically independent molecules are given. [c] The parameter in parentheses refers to compound **5**.

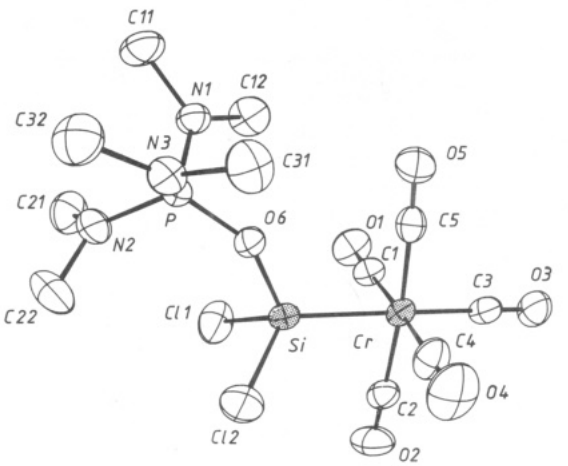

Figure 4. Molecular structure of $(OC)_5Cr{=}Si(HMPA)Cl_2$ (**8**) in the crystal.

of the different metals and the substituents at the silylene centers. The iron complexes **4** and **5**, and the chromium complexes **7** and **8** are isostructural, respectively. This illustrates that the silicon-bonded methyl groups and

Table IV. Selected Interatomic Distances (Å) and Angles (deg) in the Crystal Structures of 7 and 8

	7	8
Bond Distances		
Cr–Si	2.410 (1)	2.342 (1)
Cr–C3	1.866 (3)	1.862 (4)
Cr–C1	1.873 (3)	1.883 (4)
Cr–C2	1.883 (3)	1.893 (4)
Cr–C4	1.860 (3)	1.889 (4)
Cr–C5	1.870 (3)	1.873 (4)
Si–O6	1.743 (2)	1.690 (2)
Si–C6 (Si–Cl1)[a]	1.870 (3)	2.111 (2)
Si–C7 (Si–Cl2)[a]	1.874 (3)	2.088 (2)
P–O6	1.521 (2)	1.543 (2)
C3–O3	1.148 (4)	1.156 (5)
C1–O1	1.148 (4)	1.139 (5)
C2–O2	1.146 (4)	1.147 (5)
C4–O4	1.161 (4)	1.136 (5)
C5–O5	1.152 (4)	1.154 (5)
P–N1	1.618 (2)	1.613 (3)
P–N2	1.622 (2)	1.617 (3)
P–N3	1.626 (2)	1.617 (3)
N1–C11	1.473 (4)	1.466 (5)
N1–C12	1.446 (4)	1.448 (5)
N2–C21	1.468 (4)	1.473 (5)
N2–C22	1.463 (4)	1.454 (5)
N3–C31	1.469 (4)	1.469 (5)
N3–C32	1.470 (4)	1.461 (5)
Bond Angles		
Cr–Si–C6 (Cr–Si–Cl1)[a]	117.1 (1)	118.1 (1)
Cr–Si–C7 (Cr–Si–Cl2)[a]	117.1 (1)	119.2 (1)
C6–Si–C7 (Cl1–Si–Cl2)[a]	105.3 (2)	100.3 (1)
Cr–Si–O6	111.5 (1)	115.5 (1)
C6–Si–O6 (Cl1–Si–O6)[a]	101.7 (1)	99.7 (1)
C7–Si–O6 (Cl2–Si–O6)[a]	102.2 (1)	100.6 (1)
Si–O6–P	148.1 (1)	148.5 (2)
O6–P–N1	105.7 (1)	104.5 (2)
O6–P–N2	117.3 (1)	116.9 (2)
O6–P–N3	106.1 (1)	105.4 (2)
Si–Cr–C3	174.5 (1)	178.2 (1)
Si–Cr–C1	85.0 (1)	87.0 (1)
Si–Cr–C2	81.4 (1)	86.2 (1)
Si–Cr–C4	86.3 (1)	88.1 (1)
Si–Cr–C5	89.5 (1)	88.2 (1)
Cr–C3–O3	178.8 (3)	179.0 (4)
Cr–C1–O1	175.4 (1)	176.3 (4)
Cr–C2–O2	178.2 (3)	179.4 (4)
Cr–C4–O4	178.0 (3)	179.6 (3)
Cr–C5–O5	178.0 (3)	177.4 (3)

[a] The parameter in parentheses refers to compound 8.

Table V. Comparison of Important Structural Parameters of the $[(Me_2N)_3P{=}O]{\bullet}R_2Si{=}M(CO)_n$ Silylene Complexes 1, 3–5, and 6–8[a]

compd	M	R	M–Si	Si–O_{HMPA}	P–O	Σ[b]	lit.
1	Fe	*t*-BuO	2.289 (2)	1.730 (3)	1.524 (3)	342.1	9, 10
3	Fe	*t*-BuS	2.278 (1)	1.734 (2)	1.542 (2)	342.6	47
4[c]	Fe	Me	2.280 (1)	1.735 (3)	1.528 (3)	339.0	this work
			2.294 (1)	1.731 (3)	1.520 (3)	339.8	
5[c]	Fe	Cl	2.214 (1)	1.683 (3)	1.552 (3)	336.3	this work
			2.221 (1)	1.676 (3)	1.548 (3)	337.7	
6	Cr	*t*-BuO	2.431 (1)	1.736 (2)	1.527 (2)	342.2	10
7	Cr	Me	2.410 (1)	1.743 (2)	1.521 (2)	339.5	this work
8	Cr	Cl	2.342 (1)	1.690 (2)	1.543 (2)	337.6	this work

[a] Distances are given in angstroms and angles in degrees. [b] Sum of the three angles at the Si atom which do not include the HMPA O atom as a measure of planarity (see text). [c] Both crystallographically independent values are given.

chlorine atoms are of approximately equal volume. For **4** and **5** there are two crystallographically independent molecules in the asymmetric unit. Their molecular structures are virtually identical. Major differences arise only from different conformations of the HMPA NMe_2 groups.

As the figures show, the silicon atoms are in all cases metal-complexed. In the Fe complexes **1** and **3–5** the silylene ligands occupy an apical coordination site in the trigonal bipyramidal $Fe(CO)_4$ fragments. At the silanediyl silicon atoms a distorted tetrahedral substituent geometry is observed which results from further complexation by the oxygen atom of a HMPA molecule. It is this substituent geometry which allows the most insight into the nature of bonding in the complexes. The distortion mainly consists of surprisingly long Si–O bonds to the HMPA donors, which indicate a relatively weak coordination (see Table V for a summary of key structural features). This is augmented by the observation of large bonding angles at the HMPA O atoms which approach 150° (Tables III and IV). The bond angles at silicon fall into three distinct groups: the angles M–Si–O_{HMPA} are close to the tetrahedral standard, while the angles M–Si–R (R = Me, Cl) are rather large, approaching the sp^2 standard 120°. The angles included between the methyl or chlorine substituents at silicon, as well as the angles R–Si–O_{HMPA}, are noticeably smaller, in some cases close to 100° (Tables III and IV). In other complexes examined, the geometries vary similar to the one described or previously observed. The geometry might be taken as an incomplete adduct formation (with all angles close to the tetrahedral standard) of a previously tricoordinate silicon center M–SiR_2 with sp^2 angles. A resonance picture between an essentially nonbonding (with regard to the HMPA donor) and a strongly bound zwitterionic adduct was proposed to account for this bonding situation.[33c] As a measure of the extent of adduct formation, the sum of the three bond angles M–SiR_2 at the complexed silanediyl center might be taken, a value which is included in Table V. It is obvious that a small sum of bond angles indicates a stronger adduct formation. It should be immediately pointed out that these structural characteristics have parallels in some donor adducts of other group 14 "diyl" complexes such as the acetate adducts of silylene complexes[14] or the donor adducts of Sn(II) complexes. Also, the recently described donor adducts of silicon–carbon and silicon–nitrogen double bonds show remarkably similar structural features.[33]

The substituent geometry at silicon indicates that the electron deficit of the silanediyl ligand is not fully compensated by back-bonding from the metal center but mostly by electron donation from the donor molecule. Metal-bonded silyl groups are good σ-donors, which also holds for the HMPA-complexed silanediyl ligands. This is clearly reflected in the structures of **1** and **3–8**. The M–CO bonds to the CO groups trans to the silanediyl ligand are significantly shorter than those to the cis groups. That this effect is more pronounced for the chromium complexes than for the iron complexes is in line with the known reduced π-donor properties of the $Fe(CO)_4$ fragments at the apical coordination site of the trigonal bipyramid. As a further indication of the predominant σ-donor character of the silanediyl ligands the bending of the cis-CO groups *toward* these ligands might be noted, which is evident from the figures as well as from Tables III and IV.

The metal–silicon bonds in complexes **1** and **3–8** (Table V) are difficult to compare with the values established from the structures of a number of transition-metal silyl com-

(33) (a) Wiberg, N.; Wagner, G.; Müller, G.; Riede, J. *J. Organomet. Chem.* **1984**, *271*, 381. (b) Wiberg, N.; Schurz, K.; Reber, G.; Müller, G. *Nachr. Chem., Tech. Lab.* **1986**, *34*, 778. (c) Wiberg, N.; Wagner, G.; Reber, G.; Riede, J.; Müller, G. *Organometallics* **1987**, *6*, 35. (d) Reber, G.; Riede, J.; Wiberg, N.; Schurz, K.; Müller, G. *Z. Naturforsch.* **1989**, *44B*, 786.

Table VI. Crystal Structure Data for 4, 5, 7, and 8

	4	5	7	8
formula	$C_{12}H_{24}FeN_3O_5PSi$	$C_{10}H_{18}Cl_2FeN_3O_5PSi$	$C_{13}H_{24}CrN_3O_6PSi$	$C_{11}H_{18}Cl_2CrN_3O_6PSi$
M_r	405.249	446.085	429.409	470.24
cryst dimens, mm^3	0.20 × 0.30 × 0.50	0.30 × 0.40 × 0.45	0.25 × 0.30 × 0.40	0.20 × 0.25 × 0.35
cryst syst	monoclinic	monoclinic	monoclinic	monoclinic
space group	$P2_1/n$ (No. 14)	$P2_1/n$ (No. 14)	$P2_1/c$ (No. 14)	$P2_1/c$ (No. 14)
a, Å	8.353 (1)	8.488 (1)	8.591 (1)	8.667 (1)
b, Å	16.079 (3)	15.574 (3)	14.788 (2)	14.800 (2)
c, Å	29.158 (4)	29.595 (5)	16.925 (2)	16.568 (2)
β, deg	90.82 (1)	91.50 (1)	105.18 (1)	103.32 (1)
V, $Å^3$	3915.8	3910.9	2075.2	2068.0
Z	8	8	4	4
d_{calcd}, g/cm^3	1.375	1.515	1.374	1.510
μ(Mo Kα), cm^{-1}	9.3	12.1	7.0	9.6
F(000), e	1686	1824	896	960
T, °C	−40	−50	−50	−40
scan	ω	ω	ω	ω
scan width (in ω), deg	0.8	0.8	0.8	0.8
$((\sin\vartheta)/\lambda)_{max}$, $Å^{-1}$	0.572	0.669	0.594	0.594
hkl range	±9, +18, +34	+9, +17, ±33	+10, +17, ±20	±10, +17, +19
std rflns	100, 020, 006	400, 020, 004	300, 040, 008	500, 020, 008
rel transmissn	0.73–1.00	0.79–1.00		0.81–1.00
no. of rflns (measd/unique)	9055/6153	6899/6157	4061/3649	4053/3642
R_{int}	0.038	0.036	0.040	0.040
no. of rflns obsd ($F_o \geq 4.0\sigma(F_o)$)	4539	4526	3165	2983
H atoms (found/calcd)	15/33	20/16	22/2	14/4
no. of params refined	415	415	251	244
R^a	0.050	0.043	0.036	0.045
$R_w{}^b$	0.041	0.038	0.045	0.048
$(\text{shift/error})_{max}$	0.001	0.004	0.001	0.19
$\Delta\rho_{fin}$(max/min), $e/Å^3$	0.39/−0.43	0.42/−0.38	0.31/−0.29	0.75/−0.64

[a] $R = \sum(||F_o| - |F_c||)/\sum|F_o|$. [b] $R_w = [\sum w(|F_o| - |F_c|)^2/\sum wF_o^2]^{1/2}$; $w = 1/\sigma^2(F_o)$; function minimized $\sum w(|F_o| - |F_c|)^2$.

pounds.[34] This is due to the fact that the metal centers in the silyl compounds are inevitably in different coordination geometries and/or oxidation states. Bonds to silicon are also known to be particularly sensitive to electronegativity (polarization) effects, which are difficult to assess for molecular fragments. In the complexes **1** and **3–8** dipolar contributions to the metal–silicon bonds are expected to be rather large due to the drastically different electronic properties of the substituents at Si (^{t}BuO, ^{t}BuS, Me, Cl). An estimation only on the grounds of the Schomaker–Stevenson equation gives a bond shortening by dipolar interactions of 0.02 Å for Fe–Si and Cr–Si bonds, not accounting for any substituent effects.[35] If for a rough comparison one neglects these ionic contributions entirely, one arrives at 2.18/2.28 Å for uncomplexed $R_2Si{=}Fe/Cr$ bonds, respectively.[10] These double-bond lengths are based on estimated covalent radii of 1.11 and 1.21 Å for the zerovalent metal atoms in $Fe(CO)_4$ and $Cr(CO)_5$ fragments and a double-bond radius of 1.07 Å for silicon which is rather well established as half of the Si=Si bond lengths in West's symmetrical disilenes.[36] That the M–Si bond lengths in the complexes **1** and **3–8** are definitely longer is a clear indication of a strongly reduced double-bond character, already expected as a result from the HMPA complexation. However, it should also be noted at this point that an ab initio calculation for $(OC)_5Cr{=}Si(OH)H$ yields 2.4 Å for the bond in question.[37] In any event, the M–Si bonds in **1** and **3–8** are clearly affected by the substituents at silicon. As Table V shows, the M–Si bonds are very similar for the *t*-BuO, *t*-BuS, and Me substituents but drastically shorter for the chlorine-substituted silanediyls. This indicates that the electronic effects of the first three groups should be rather similar; i.e., the *t*-BuO group in particular should act predominantly as a π-donor. This could already be inferred from the large bond angles Si–O–CMe_3 of 143.7 (3)/134.5 (4)° for **1** and 142.7 (2)/132.8 (2)° for **6**, the differences being clearly due to steric effects of the bulky *t*-Bu groups.

The electron-withdrawing chlorine atoms, on the other hand, render the silicon centers particularly electron deficient, which is in part compensated for by a noticeably stronger HMPA complexation (see the shorter $Si{-}O_{HMPA}$ bonds, the longer HMPA P–O bonds, and the more pronounced pyramidalization at Si, as listed in Table V). The drastic reduction in M–Si bond lengths also points to an increase in back-bonding from the respective metal centers.[38] Unfortunately, this effect is not reflected in longer $M{-}CO_{trans}$ bonds which are of comparable lengths if the standard deviations are properly taken into account. Again, the slightly greater relative M–Si bond shortening observed for the chromium complexes might be attributed to the better π-donor properties of the $Cr(CO)_5$ fragment.

The observations on the donor-complexed silanediyl complexes **1** and **3–8** may be summarized as follows: Electronic unsaturation of the metal-complexed silanediyls leads to the addition of a nucleophile (HMPA) to the tricoordinated silicon, resulting in a distorted tetrahedral coordination geometry. The amount of distortion indicates the degree to which the addition of the nucleophile has

(34) (a) Vancea, L.; Bennett, M. J.; Jones, C. E.; Smith, R. A.; Graham, W. A. G. *Inorg. Chem.* **1977**, *16*, 897. (b) Schubert, U.; Rengstl, A. *J. Organomet. Chem.* **1979**, *166*, 323. (c) Schubert, U.; Kraft, G.; Walther, E. Z. *Z. Anorg. Allg. Chem.* **1984**, *519*, 96. (d) Knorr, M.; Müller, J.; Schubert, U. *Chem. Ber.* **1987**, *120*, 879. (e) Roddick, D. M.; Tilley, D. T.; Rheingold, A. L.; Geib, S. J. *J. Am. Chem. Soc.* **1987**, *109*, 945 and references cited therein.

(35) Schomaker, V.; Stevenson, D. P. *J. Am. Chem. Soc.* **1941**, *63*, 1368. This estimation is based on the following parameters: r_{Si} = 1.07 Å, r_{Fe} = 1.11 Å, r_{Cr} = 1.21 Å, X_{Si} = 1.74, X_{Fe} = 1.80, X_{Cr} = 1.56.

(36) West, R. *Angew. Chem.* **1987**, *99*, 1231; *Angew. Chem., Int. Ed. Engl.* **1987**, *26*, 1201.

(37) Nakatsuji, H.; Ushio, J.; Yonezawa, T. *J. Organomet. Chem.* **1983**, *258*, C1.

(38) Small covalent radii for chlorine-substituted silicon atoms have been observed previously: Hönle, W.; von Schnering, H. G. *Z. Anorg. Allg. Chem.* **1980**, *464*, 139.

Table VII. Fractional Atomic Coordinates and Equivalent Isotropic Displacement Parameters for 4

atom	x/a	y/b	z/c	U_{eq},[a] Å^2
Fe	−0.00183 (7)	0.24973 (4)	0.01750 (2)	0.032
O1	0.1821 (5)	0.0956 (2)	0.0141 (1)	0.073
C1	0.1079 (7)	0.1561 (3)	0.0150 (2)	0.048
O2	−0.1946 (4)	0.2856 (2)	0.0977 (1)	0.055
C2	−0.1187 (6)	0.2716 (3)	0.0656 (2)	0.039
O3	−0.2753 (5)	0.1978 (3)	−0.0396 (1)	0.088
C3	−0.1685 (7)	0.2179 (3)	−0.0177 (2)	0.052
O4	0.1071 (4)	0.3871 (2)	−0.0396 (1)	0.050
C4	0.0626 (5)	0.3325 (3)	−0.0170 (2)	0.036
Si	0.2069 (1)	0.29079 (8)	0.06335 (4)	0.029
C5	0.2273 (7)	0.2348 (3)	0.1190 (2)	0.058
C6	0.4073 (6)	0.2917 (3)	0.0358 (2)	0.051
P1	0.2525 (1)	0.46680 (7)	0.10697 (4)	0.030
O5	0.1810 (3)	0.3931 (2)	0.08075 (9)	0.033
N1	0.1004 (4)	0.5177 (2)	0.1250 (1)	0.035
C11	0.1216 (6)	0.6014 (3)	0.1434 (2)	0.061
C12	−0.0624 (6)	0.4872 (3)	0.1271 (2)	0.046
N2	0.3627 (4)	0.5190 (2)	0.0714 (1)	0.034
C21	0.4817 (6)	0.5804 (3)	0.0863 (2)	0.055
C22	0.2964 (6)	0.5362 (3)	0.0255 (2)	0.049
N3	0.3689 (4)	0.4443 (2)	0.1498 (1)	0.035
C31	0.3094 (7)	0.4360 (4)	0.1963 (2)	0.063
C32	0.5295 (6)	0.4097 (3)	0.1445 (2)	0.054
Fe′	−0.49676 (7)	0.25332 (4)	−0.21635 (2)	0.030
O1′	−0.6625 (6)	0.4108 (2)	−0.2015 (1)	0.068
C1′	−0.5955 (6)	0.3479 (3)	−0.2068 (2)	0.043
O2′	−0.2903 (4)	0.1800 (3)	−0.1460 (1)	0.079
C2′	−0.3737 (6)	0.2086 (3)	−0.1737 (2)	0.047
O3′	−0.2257 (5)	0.3203 (3)	−0.2673 (1)	0.078
C3′	−0.3338 (6)	0.2950 (3)	−0.2478 (2)	0.048
O4′	−0.6312 (5)	0.1497 (2)	−0.2894 (1)	0.072
C4′	−0.5765 (6)	0.1903 (3)	−0.2601 (2)	0.041
Si′	−0.6994 (1)	0.19975 (8)	−0.17306 (4)	0.030
C5′	−0.7241 (6)	0.2444 (3)	−0.1149 (2)	0.055
C6′	−0.8996 (6)	0.1977 (3)	−0.2016 (2)	0.051
P1′	−0.7198 (2)	0.01330 (7)	−0.14296 (4)	0.032
O5′	−0.6599 (3)	0.0964 (2)	−0.16073 (9)	0.033
N1′	−0.9109 (5)	0.0014 (2)	−0.1390 (1)	0.039
C11′	−1.0010 (6)	0.0358 (3)	−0.1007 (2)	0.054
C12′	−1.0125 (7)	−0.0240 (3)	−0.1773 (2)	0.061
N2′	−0.6505 (5)	0.0033 (2)	−0.0913 (1)	0.040
C21′	−0.6988 (7)	−0.0656 (3)	−0.0611 (2)	0.055
C22′	−0.5044 (7)	0.0439 (4)	−0.0752 (2)	0.070
N3′	−0.6592 (5)	−0.0531 (2)	−0.1809 (1)	0.045
C31′	−0.5428 (8)	−0.0336 (4)	−0.2145 (2)	0.082
C32′	−0.6824 (9)	−0.1422 (3)	−0.1745 (2)	0.073

[a] $U_{eq} = {}^1/_3\sum_i\sum_j U_{ij}a^*_i a^*_j \mathbf{a}_i\cdot\mathbf{a}_j$.

proceeded. This degree is a function of the electronic saturation at silicon, which is in large part influenced by the substituents at silicon. A highly electron-deficient silicon leads to a stronger coordination of the donor and to a stronger pyramidalization and vice versa. Backbonding from the metal centers also compensates for the electron deficiency at silicon but plays a minor role. The molecular structures definitely indicate a large σ-donor character of the complexed silanediyls; the π-acceptor properties are reduced with respect to those of carbene complexes. Shorter M–Si bonds have to be expected for uncomplexed (donor-free) silanediyl transition-metal complexes with the substituent geometry at the unsaturated silicon atom close to trigonal planar.

Molecular Orbital Description

The observed effects can be rationalized by a qualitative molecular orbital description. A detailed discussion is given in ref 10, but some arguments are summarized for the purpose of comparison: The fragment orbitals of $Cr(CO)_5$ and $Fe(CO)_4$ are depicted in Figure 5. A (base-free) metal–silicon double bond is formed by interaction of the a_1 (3s) orbital of the silylene with the empty a_1 (d_{z^2})

Table VIII. Fractional Atomic Coordinates and Equivalent Isotropic Displacement Parameters for 5

atom	x/a	y/b	z/c	U_{eq}, Å^2
Fe	0.01414 (7)	0.25222 (4)	0.01859 (2)	0.035
O1	0.1909 (5)	0.0912 (2)	0.0161 (1)	0.078
C1	0.1220 (6)	0.1546 (3)	0.0172 (2)	0.052
O2	−0.1901 (4)	0.2963 (2)	0.0932 (1)	0.066
C2	−0.1106 (5)	0.2785 (3)	0.0639 (2)	0.043
O3	−0.2461 (5)	0.1916 (3)	−0.0404 (1)	0.085
C3	−0.1438 (6)	0.2150 (3)	−0.0177 (2)	0.053
O4	0.1088 (4)	0.3939 (2)	−0.0398 (1)	0.054
C4	0.0729 (5)	0.3372 (3)	−0.0173 (2)	0.042
Si	0.2079 (1)	0.29784 (7)	0.06406 (4)	0.031
Cl1	0.2403 (2)	0.23535 (8)	0.12578 (4)	0.062
Cl2	0.4337 (1)	0.29551 (9)	0.03843 (4)	0.055
P1	0.2655 (1)	0.47695 (7)	0.10736 (4)	0.032
O5	0.1904 (3)	0.4006 (2)	0.08090 (9)	0.037
N1	0.1163 (4)	0.5303 (2)	0.1242 (1)	0.038
C11	0.1353 (6)	0.6195 (3)	0.1386 (2)	0.058
C12	−0.0415 (6)	0.4958 (3)	0.1322 (2)	0.051
N2	0.3712 (4)	0.5291 (2)	0.0721 (1)	0.038
C22	0.3079 (6)	0.5461 (3)	0.0266 (2)	0.049
C21	0.5000 (6)	0.5886 (3)	0.0855 (2)	0.059
N3	0.3805 (4)	0.4512 (2)	0.1495 (1)	0.040
C31	0.3225 (6)	0.4434 (3)	0.1953 (2)	0.062
C32	0.5328 (6)	0.4083 (3)	0.1429 (2)	0.059
Fe′	−0.50855 (7)	0.25168 (4)	−0.21623 (2)	0.033
O1′	−0.6743 (5)	0.4139 (2)	−0.2035 (1)	0.071
C1′	−0.6084 (6)	0.3500 (3)	−0.2083 (1)	0.044
O2′	−0.2949 (4)	0.1769 (3)	−0.1478 (1)	0.074
C2′	−0.3795 (5)	0.2058 (3)	−0.1750 (2)	0.044
O3′	−0.2465 (5)	0.3282 (3)	−0.2642 (1)	0.083
C3′	−0.3483 (6)	0.2985 (3)	−0.2461 (2)	0.049
O4′	−0.6216 (5)	0.1451 (3)	−0.2917 (1)	0.079
C4′	−0.5774 (6)	0.1864 (3)	−0.2620 (2)	0.048
Si′	−0.6992 (1)	0.19220 (7)	−0.17685 (4)	0.031
Cl1′	−0.7522 (2)	0.24404 (8)	−0.11433 (4)	0.057
Cl2′	−0.9216 (1)	0.18427 (8)	−0.20791 (4)	0.056
P1′	−0.7219 (1)	0.00508 (7)	−0.14184 (4)	0.036
O5′	−0.6619 (3)	0.0900 (2)	−0.16238 (9)	0.035
N1′	−0.9085 (4)	−0.0054 (2)	−0.1372 (1)	0.044
C11′	−0.9923 (6)	0.0356 (4)	−0.1006 (2)	0.064
C12′	−1.0134 (6)	−0.0348 (4)	−0.1748 (2)	0.067
N2′	−0.6454 (4)	0.0006 (2)	−0.0915 (1)	0.045
C21′	−0.6877 (7)	−0.0677 (3)	−0.0599 (2)	0.061
C22′	−0.5045 (7)	0.0457 (4)	−0.0769 (2)	0.087
N3′	−0.6665 (5)	−0.0660 (2)	−0.1778 (1)	0.056
C31′	−0.5447 (8)	−0.0511 (4)	−0.2089 (3)	0.101
C32′	−0.690 (1)	−0.1574 (3)	−0.1675 (2)	0.102

Table IX. Fractional Atomic Coordinates and Equivalent Isotropic Displacement Parameters for 7

atom	x/a	y/b	z/c	U_{eq}, Å^2
Cr	0.03728 (5)	0.17288 (3)	0.94508 (3)	0.029
C1	−0.1269 (4)	0.0952 (2)	0.8890 (2)	0.038
O1	−0.2292 (3)	0.0514 (2)	0.8503 (2)	0.059
C2	−0.0009 (4)	0.1447 (2)	1.0469 (2)	0.041
O2	−0.0258 (4)	0.1299 (2)	1.1089 (1)	0.065
C3	0.1987 (4)	0.0857 (2)	0.9564 (2)	0.040
O3	0.2962 (3)	0.0310 (2)	0.9637 (2)	0.062
C4	0.1765 (4)	0.2658 (2)	0.9924 (2)	0.045
O4	0.2610 (3)	0.3255 (2)	1.0201 (2)	0.073
C5	0.0490 (3)	0.2143 (2)	0.8424 (2)	0.035
O5	0.0513 (3)	0.2398 (2)	0.7784 (1)	0.053
Si	−0.17819 (9)	0.27843 (5)	0.94143 (4)	0.030
C6	−0.3788 (4)	0.2300 (3)	0.9423 (2)	0.052
C7	−0.1388 (5)	0.3697 (3)	1.0211 (2)	0.058
O6	−0.2261 (2)	0.3405 (1)	0.8507 (1)	0.038
P	−0.34714 (8)	0.39983 (5)	0.79136 (4)	0.026
N1	−0.4031 (3)	0.3422 (2)	0.7074 (1)	0.035
C11	−0.4970 (5)	0.3867 (2)	0.6321 (2)	0.050
C12	−0.3524 (5)	0.2511 (2)	0.6959 (2)	0.055
N2	−0.5091 (3)	0.4287 (2)	0.8173 (1)	0.034
C21	−0.6599 (4)	0.3770 (3)	0.7926 (2)	0.048
C22	−0.5059 (5)	0.4938 (2)	0.8829 (2)	0.053
N3	−0.2543 (3)	0.4943 (2)	0.7850 (1)	0.033
C31	−0.0840 (4)	0.4917 (2)	0.7837 (2)	0.045
C32	−0.3370 (4)	0.5778 (2)	0.7499 (2)	0.051

Table X. Fractional Atomic Coordinates and Equivalent Isotropic Displacement Parameters for 8

atom	x/a	y/b	z/c	U_{eq}, Å^2
Cr	0.01698 (7)	0.17895 (4)	0.94690 (4)	0.033
C1	−0.1350 (5)	0.0956 (3)	0.8915 (2)	0.041
O1	−0.2268 (4)	0.0474 (2)	0.8541 (2)	0.065
C2	−0.0237 (5)	0.1473 (3)	1.0507 (3)	0.044
O2	−0.0488 (5)	0.1288 (2)	1.1138 (2)	0.070
C3	0.1787 (5)	0.0940 (3)	0.9566 (2)	0.042
O3	0.2775 (4)	0.0403 (2)	0.9622 (2)	0.062
C4	0.1566 (5)	0.2711 (3)	0.9981 (3)	0.050
O4	0.2407 (5)	0.3262 (2)	1.0292 (3)	0.083
C5	0.0407 (5)	0.2182 (3)	0.8429 (3)	0.039
O5	0.0493 (4)	0.2415 (2)	0.7777 (2)	0.058
Si	−0.1916 (1)	0.28228 (7)	0.93545 (6)	0.035
Cl1	−0.4188 (1)	0.23149 (9)	0.93616 (8)	0.065
Cl2	−0.1733 (2)	0.3857 (1)	1.02288 (8)	0.079
O6	−0.2358 (3)	0.3425 (2)	0.8465 (1)	0.037
P	−0.3549 (1)	0.40275 (6)	0.78629 (5)	0.030
N1	−0.3975 (4)	0.3461 (2)	0.7009 (2)	0.038
C11	−0.4836 (6)	0.3901 (3)	0.6244 (2)	0.054
C12	−0.3595 (6)	0.2521 (3)	0.6905 (3)	0.054
N2	−0.5170 (4)	0.4287 (2)	0.8135 (2)	0.040
C21	−0.6633 (5)	0.3751 (3)	0.7880 (3)	0.056
C22	−0.5185 (6)	0.4891 (3)	0.8825 (3)	0.058
N3	−0.2638 (4)	0.4974 (2)	0.7825 (2)	0.036
C31	−0.0926 (5)	0.4984 (3)	0.7867 (3)	0.052
C32	−0.3445 (6)	0.5811 (3)	0.7503 (3)	0.054

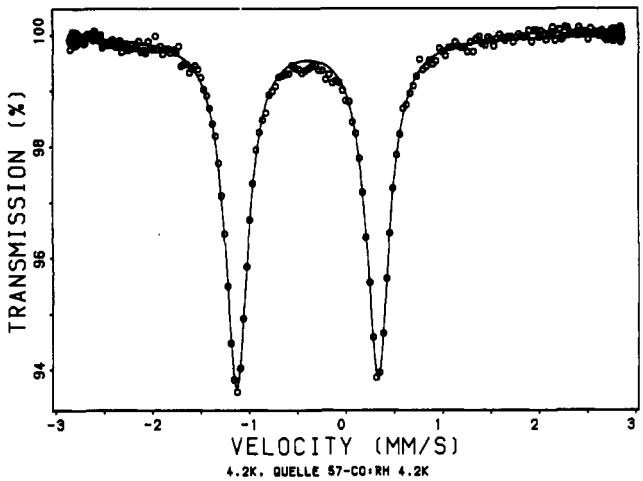

Figure 5. Mössbauer spectrum of $(OC)_4Fe{=}Si(HMPA)(t\text{-}BuO)_2$ (1) at 4.2 K (source ^{57}Co:Rh, Fe metal as standard).

orbitals of the respective metal fragments. π-Bonding occurs basically by interaction of the filled e_s (d_{yz}, d_{xz}) orbitals at the metal with the empty b_1 (p) orbital at silicon.

An ab initio calculation for $(OC)_5Cr{=}Si(OH)H$ shows that silicon is highly electron deficient.[37] The Cr=Si bond dissociation energy to the singlet fragments $Cr(CO)_5$ and Si(OH)H is 29.6 kcal/mol, compared to 44.4 kcal/mol for the carbene complex analogue $(OC)_5Cr{=}C(OH)H$. The results indicate that the silicon–metal double bond should be more labile than the corresponding C=M double bonds, which is quite the reverse of the known stabilities of the respective single bonds. The gross atomic charges are 0.87 at Cr and −0.06 at Si and 0.80 at Cr and −0.19 at C for the carbene complex. The LUMO of $(CO)_5Cr{=}Si(OH)H$ is π-antibonding between Cr and Si with a maximum coefficient of 0.85 at Si and an orbital energy of 2.12 eV. The values for $(OC)_5Cr{=}C(OH)H$ are 0.66 for the coefficient at C with an orbital energy of 3.86 eV.[37] This electron deficiency at silicon leads, together with the undercoordination, to the additional fixation of a donor molecule. The electronic interaction of the donor occurs with the LUMO (π-antibonding) of the π-bond; thus, a stronger coordination of the donor leads to an elongation of the metal–silicon bond and an increased pyramidalization effect at silicon.

Table XI. MNDOG Calculation Results for the Silylenes (Silanediyls) $Si(OMe)_2$, $SiMe_2$, and $SiCl_2$

	$Si(OMe)_2$		
heat of formation, kcal/mol	−127.529 00		eigenvalues, eV
			−42.431 28
total energy, eV	−1074.787 43		−40.293 64
ionization potential, eV	9.026 58		−27.561 53
dipole moment, D	0.274 96		−27.173 47
net atomic charges			−18.292 83
Si	1.068 96		−17.282 61
O	−0.727 73		−15.418 79
			−15.096 36
geometry			−15.002 36
Si–O, Å	1.6329		−11.573 52
bond angle O–Si–O, deg	102.402		−11.501 70
O–C, Å	1.3594		−10.995 72
bond angle C–O–Si, deg	148.028		−10.879 91
twist angle C–O–Si–O, deg	299.664	HOMO	−9.026 58
		LUMO	1.277 64
	$SiMe_2$		
heat of formation, kcal/mol	30.80191		eigenvalues, eV
total energy, eV	−427.01933		−32.84575
ionization potential, eV	7.50334		−28.94187
dipole moment, D	0.73387		−14.12721
			−14.10033
net atomic charges			−13.91588
Si	0.73232		−13.72629
C	−0.36475		−13.65485
			−11.15905
geometry			−7.50334
Si–C, Å	1.7962	HOMO	0.03950
bond angle C–Si–C, deg	105.906	LUMO	
	$SiCl_2$		
heat of formation, kcal/mol	−46.29454		eigenvalues, eV
total energy, eV	−798.29658		−25.13072
ionization potential, eV	9.82554		−24.11956
dipole moment, D	4.18054		−18.23527
			−14.22343
net atomic charge			−13.17479
Si	1.15634		−13.14839
Cl	−0.57817		−12.69826
			−12.45147
geometry			−9.82554
Si–Cl, Å	2.0880	HOMO	−1.02425
bond angle, deg	105.469	LUMO	

The results of a MNDO calculation of the free silylenes provide a further rationalization of the observed trends of the metal–silicon bond lengths. Silylenes have been calculated on high quantum-mechanic levels by ab initio methods and with extended basis sets. The purpose of this MNDO calculation is to obtain comparable results for silylenes $Si(OMe)_2$, $SiMe_2$, and $SiCl_2$ from the same method; $Si(t\text{-}BuO)_2$ has been approximated by $Si(OMe)_2$.

For a series of complexes with varying substituents *t*-BuO, Me, and Cl and the metal fragments $Fe(CO)_4$ and $Cr(CO)_5$, the frontier orbital energies and electron densities of the free silylenes can also be taken as an indicator for the electronic situation of the coordination compound. The energies of the LUMO's drop from 1.2776 eV for $Si(OMe)_2$ to −0.3950 eV for $SiMe_2$ to −1.024 eV for $SiCl_2$. This situation is the basis for an increasing π-back-bonding capacity M–Si from $Si(OMe)_2$ through $SiMe_2$ to $SiCl_2$. The energies of the HOMO's also follow the same trend, as well as the net atomic charges at silicon and the dipole moments; however, $SiCl_2$ plays a special role because of its high polarity (Table XI). The silicon atom in the oxo-silanediyl complexes is saturated by O–Si π-interaction and in the methyl complexes by a strong hyperconjugative effect. In the chloro complexes the polarity for $SiCl_2$ (dipole moment) presumably leads also to a rather high charge separation in the coordination compounds and a significant shortening of the metal–silicon bonds by dipolar contributions.

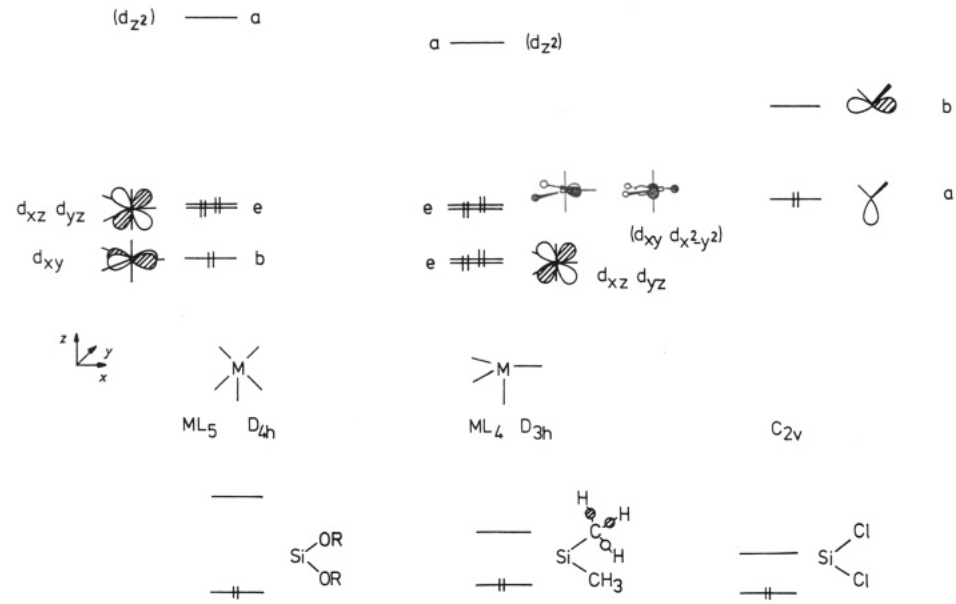

Figure 6. Valence orbitals of the fragments $[Fe(CO)_4]$ and $[Cr(CO)_5]$.

The observed M–Si bond lengths vary much less with changing substituents for iron than for chromium. This reflects the reduced π-donor capacity of the $Fe(CO)_4$ fragment at the axial coordination site of the trigonal bipyramid compared to the $Cr(CO)_5$ case. It can be shown by data from PE spectroscopy that the highest occupied orbital t_{2g} in $Cr(CO)_6$ is higher in energy by 1.19 eV than the respective set of two degenerate e orbitals in $Fe(CO)_5$.[39] This situation leads to a much more zwitterionic structure in the case of the iron complexes, which is in accordance with the physical properties (solubility, melting point, etc.) of the compounds.

To summarize the observed trends, addition of a nucleophile (HMPA) to a tricoordinated silicon leads to a distorted tetrahedral coordination geometry. The degree of distortion indicates the stage to which the addition of the nucleophile to silicon has proceeded. The addition process is a function of the electronic saturation at silicon and is strongly influenced by the electronic properties of the substituents. A highly electron deficient silicon leads to a stronger coordination of the donor and to a stronger pyramidalization and vice versa.

The observed structures represent model cases for the consecutive stages of a nucleophilic addition reaction to a trigonal planar silicon along a presumed reaction coordinate.

Electrochemical Investigations

Cyclic voltammograms of **1** and **4** have been measured at room temperature in THF at Pt electrodes under nitrogen (with added n-$Bu_4N^+Cl^-$ for conductivity) with a Ag/AgCl electrode as standard (3 M KCl). The data show both irreversible oxidation (+725 mV, **1**; +962 mV, **4**) and reduction potentials (−1.318 mV, **1**; −1.280 mV, **4**). The compounds **1** and **4** can also be oxidized by ferrocene.

The observed redox potentials correlate with the expected electron densities at silicon. Further investigations are under way, and a detailed description of the electrochemical properties of the complexes together with their redox chemistry will be given elsewhere.

Table XII. Mössbauer Data for Iron Silylene Complexes (Fe as Standard)

compd	IS/mm s^{-1}	QS/mm s^{-1}
$(OC)_4FeSi(HMPA)_2Fe(CO)_4$	−0.488	1.62
$(OC)_4FeSi(HMPA)(t\text{-}BuO)_2$	−0.477	1.46
$Na_2Fe(CO)_4$[a,b]	−0.328	
$Fe(CO)_5$[a,c]	−0.178	

[a] Goldanski, V. I., Herber, R. H., Eds. *Chemical Applications of Mössbauer Spectroscopy*; Academic Press: New York, 1968. [b] T = 298 K. [c] T = 78 K.

Mössbauer Spectroscopy

A further experimental indicator for the amount of charge transfer from silicon to iron is provided by Mössbauer spectroscopy. The spectra for the compounds **1** and **20** have been measured at 4.2 K and show the isomeric shifts IS = −0.477 mm s^{-1} (**1**) and IS = −0.488 mm s^{-1} (**20**) with the respective quadrupole splitting QS = 1.46 mm (**1**) and QS = 1.62 mm (**20**) (Table XII, Figure 6). A comparable value for iron(−II) in $Na_2Fe(CO)_4$ is −0.328 mm s^{-1}. The observed quadrupole splitting is normal for a trigonal bipyramidal d^8 system, but the negative isomer shifts have no precedent in the literature and indicate a relatively high electron density at the iron atom. This effect can be rationalized by the superior σ-acceptor capacity of the $Fe(CO)_4$ fragment at the axial coordination site.[40] It should be noted, however, that the spectroscopic data for the CO ligands provide no indication for unusually high electron density on the $Fe(CO)_4$ fragment.

Force Field Calculations and Steric Effects

Force field calculations on the complexes **1** and **4–8** reproduce the conformation found in the crystal as the global energy minimum. The potential energy of the molecules was minimized as the sum of vibrational energy and van der Waals interactions. All introduced parameters are listed in the Experimental Section. The metal atoms were assumed to be quasi-rigid coordination centers with increased force constants for the bending modes ν(M–CO). This measure was necessary in order to establish the

(39) Böhm, M. C.; Daub, J.; Gleiter, R.; Hofmann, P.; Lappert, M. F.; Öfele, K. *Chem. Ber.* **1980**, *113*, 3629.

(40) (a) Pebler, J.; Petz, W. *Z. Naturforsch.* **1977**, *32B*, 1431–1434. (b) Pannell, K. H.; Liu, S. H.; Kapoor, R. N.; Cervantes-Lee, F.; Pinon, M.; Parkayi, L. *Organometallics* **1990**, *9*, 2453–2462.

Table XIII. Energies in kcal/mol and Selected Bond Distances in Å and Bond Angles in deg for the Complexes 1 and 4–8 Obtained by Force Field Calculation

	6, Cr-*t*-Bu	7, CrMe	8, CrCl	1, Fe-*t*-Bu	4, FeMe	5, FeCl
Energies						
E_{tot}	43.4	45.7	31.7	28.0	54.0	29.5
E_{bond}	8.0	14.8	5.8	7.6	17.0	6.8
E_{angle}	31.5	31.3	25.0	19.8	31.1	21.0
E_{tors}	17.5	8.3	8.4	14.6	8.0	6.0
E_{VdW}	-13.6	-8.7	-7.5	-14.0	-2.1	-4.3
Bond Distances and Angles						
	(t-BuO)$_2$(HMPA)Si=Cr(CO)$_5$ (6)					
Cr-Si	2.405	Cr-Si-O1	108.0			
Si-O1	1.725	Cr-Si-O2	117.4			
Si-O2	1.737	O2-Si-O2	105.5			
Si-O3	1.732	sum	330.9			
	Me$_2$(HMPA)Si=Cr(CO)$_5$ (7)					
Cr-Si	2.428	Cr-Si-Me	112.6			
Si-Me	1.237	Cr-Si-Me	113.4			
Si-Me	1.236	Me-Si-Me	111.7			
Si-O	1.729	sum	337.7			
	Cl$_2$(HMPA)Si=Cr(CO)$_5$ (8)					
Cr-Si	2.403	Cr-Si-Cl	109.5			
Si-Cl	1.089	Cr-Si-Cl	111.1			
Si-Cl	1.087	Cl-Si-Cl	109.1			
Si-O	1.698	sum	329.7			
	(t-BuO)$_2$(HMPA)Si=Fe(CO)$_4$ (1)					
Fe-Si	2.303	Fe-Si-O1	110.2			
Si-O1	1.711	Fe-Si-O2	111.3			
Si-O2	1.708	O1-Si-O2	110.9			
Si-O3	1.717	sum	332.4			
	Me$_2$Si(HMPA)Si=Fe(CO)$_4$ (4)					
Fe-Si	2.323	Fe-Si-Me	113.4			
Si-Me	1.235	Fe-Si-Me	114.6			
Si-Me	1.259	Me-Si-Me	112.2			
Si-O	1.738	sum	340.2			
	Cl$_2$Si(HMPA)Si=Fe(CO)$_4$ (5)					
Fe-Si	2.300	Fe-Si-Cl	111.4			
Si-Cl	1.091	Fe-Si-Cl	109.8			
Si-Cl	1.087	Cl-Si-Cl	108.9			
Si-O	1.708	sum	330.1			

trigonal bipyramidal coordination geometry at iron. Otherwise, calculations for pentacoordinated complexes LM(CO)$_4$ with a large substituent L, on the basis of a force field, only lead to square pyramidal structures with the four CO's forming the base of a pyramid as the sterically most favored situation. Our model of quasi-rigid coordination centers accounts for the electronic preference of a trigonal bipyramidal coordination geometry in the d^8 iron complexes. The structures obtained match the observed conformations with minor deviations from the solid-state structures. The calculations underestimate the deviations from tetrahedral geometry at silicon found in the crystal structures, which result from electronic rather from steric effects. Furthermore, the observed slight inclination of the coordinated CO's toward the silicon atom is not reproduced. However, the relative orientation (rotamers) of the *t*-BuO groups is (Figure 7, Table XIII) clearly established as the global potential energy minimum due to steric interactions in the molecule. Packing effects of the lattice obviously play a minor role. For compounds 1 and 6, the calculations indicate attractive van der Waals forces between the *tert*-butoxy substituents (Table XIII). These arguments allow the conclusion that the *tert*-butoxy groups form an ideal constellation for a perfect shielding of the silicon atom in 1 and 6.

With the introduction of reasonable boundary conditions, in the cases discussed force field calculations provide a good basis for the separation of steric from electronic effects. Metal–silicon bond lengths and pyramidalization at silicon are a function of electronic effects. The particular orientation of the organic substituents at silicon is, however, predominantly influenced by steric interactions.

Reactions of Base-Stabilized Silylene Complexes

Silylene Complexes as Silylene Sources. Relatively few reports are known concerning the reactivity of silylene complex base adducts. Tilley has recently reported the reduction of **17** with $LiAlH_4$ together with its hydrolysis reaction, as well as some derivatization reactions with alcohols, ketones, and acetic acid; however, no further transfer reactions of the coordinated silylenes are known.[41]

Complexes **5–7** show an interesting photochemistry which leads to cleavage and transfer of the silylenes to organic substrates such as 2,3-dimethylbutadiene. These reactivities clearly document the potential of the silylene complexes to react as a silylene source.

Photolysis of **1**, **4**, and **6** in the presence of triphenylphosphine proceeds in two steps, yielding the trans-phosphine complexes **25** (eq 5) and **27** (eq 6) by stepwise displacement of CO and the silylene ligand. The trans-phosphine/silylene complexes **23** and **24** (eq 5) and **26** (eq 6) are isolable intermediates.

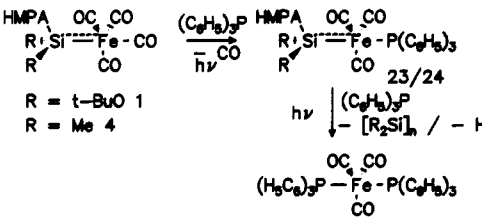

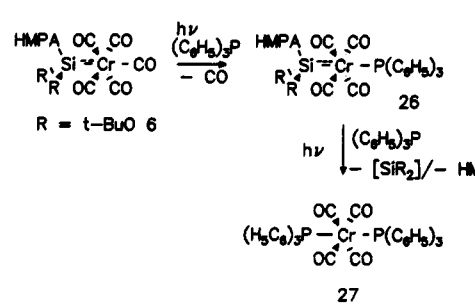

The CO displacement reaction **1** → **23** follows the second-order rate law $-d[23]/dt = [1][(C_6H_5)_3P]$ with $k = (8.9 \pm 0.5) \times 10^{-3}$ mol s^{-1} at −40.0 (±1.0) °C with a quantum yield $\Phi = 0.021$ (254 nm).[42] The CO displacement reaction can be suppressed by an excess of CO. These experiments support a dissociative reaction pathway through a highly reactive 16e$^-$ species as intermediate. The coordination of the phosphine to the 16e$^-$ complex can be considered to be the rate-determining step.[43]

Further photolysis of **23** and **24** (eq 5) or **26** (eq 6) in the presence of an excess of phosphine leads to the *trans*-bis(phosphine) carbonyl complexes **25** and **27** by displacement of the silylenes.[12] Concomitant with this process, HMPA is liberated and polysilanes are formed. The polysilanes have been isolated and identified by spectroscopic methods ($[Me_2Si]_n$, ^{29}Si NMR δ −22, ^{1}H NMR δ 0.2 (br), MS (EI) *m/e* 420, M_r (dioxane) 550 (±10); [(*t*-

(41) Zhang, C.; Grumbine, S. D.; Tilley, T. D. *Polyhedron* **1991**, *10*, 1173.

(42) The reaction rate has been measured for two different phosphine and silylene complex concentrations.

(43) Klassen, J. K.; Selke, M.; Sorensen, A. A.; Yang, G. K. In *Bonding Energetics in Organometallic Compounds*; Marks, T. J., Ed.; ACS Symposium Series 428; American Chemical Society: Washington, DC, 1990.

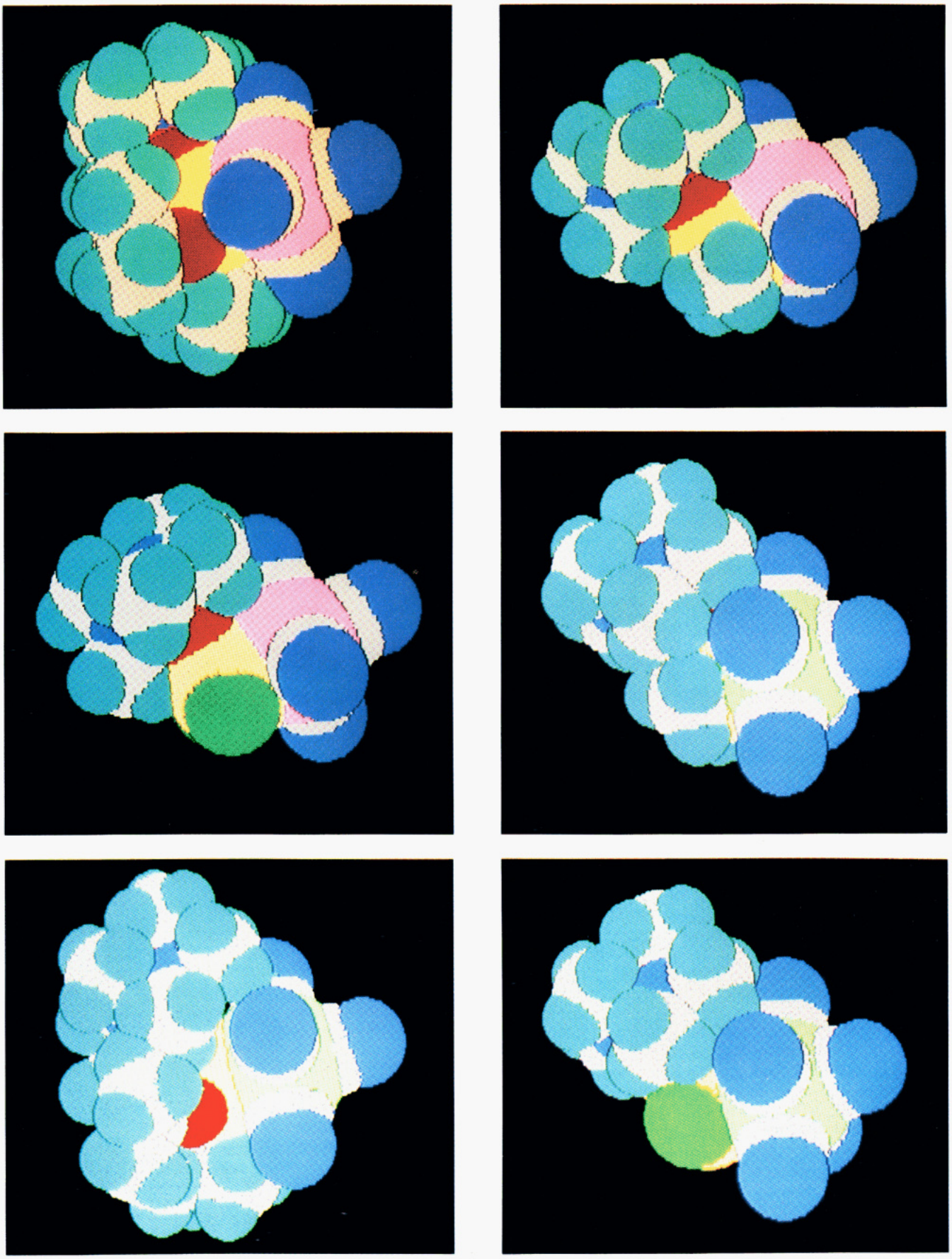

Figure 7. Picture of the van der Waals radii obtained by force field calculation of the complexes (a, top left) $(OC)_4Fe{=}Si(HMPA)(t\text{-}BuO)_2$ (**1**), (b, top right) $(OC)_4Fe{=}Si(HMPA)Me_2$ (**4**), (c, middle left) $(OC)_4Fe{=}Si(HMPA)Cl_2$ (**5**), (d, middle right) $(OC)_5Cr{=}Si(HMPA)Me_2$ (**7**), (e, bottom left) $(OC)_5Cr{=}Si(HMPA)(t\text{-}BuO)_2$ (**6**), and (f, bottom right) $(OC)_5Cr{=}Si(HMPA)Cl_2$ (**8**).

$BuO)_2Si]_n$, ^{29}Si NMR −71.2 (br), ^1H NMR δ 1.2 (br)).[44]

Furthermore, heating of $Me_2Si(HMPA)=Fe(CO)_4$ up to 110 °C at 10^{-4} bar leads to loss of HMPA and formation of the dimeric complex **22** (^{29}Si NMR 159 ppm; eq 7). Prolonged heating of **22** at 150 °C yields also small amounts (3%) of dimethylpolysilane along with a mixture of iron carbonyl cluster compounds.

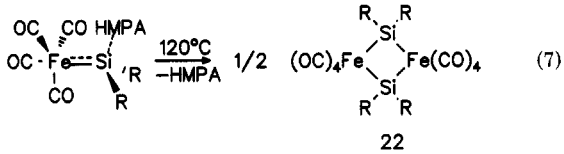

(7)

22

Polysilanes are obtainable by different routes: by photochemical base-assisted displacement of silylenes and by thermal treatment of silylenes complexes. Furthermore, cleavage of silylene complexes with pyridine is also possible.[45,46] Polysilane formation has been observed for the metals Fe and Cr and the substituents *t*-BuO, *t*-BuS, and Me at silicon.

Trapping of Silylenes by 2,3-Dimethylbutadiene. The silylenes presumably polymerize in solution after being split off from the metal. Evidence for such a mechanism is provided by trapping experiments: Cophotolysis of the complex **1** with a 10-fold excess of 2,3-dimethylbutadiene yields the silacyclopentene **28** and (2,3-dimethylbutadiene)iron tricarbonyl (**29**). **28** and **29** have been isolated (eq 8). The reactions described show that silylene complexes decompose quantitatively to form silylenes.

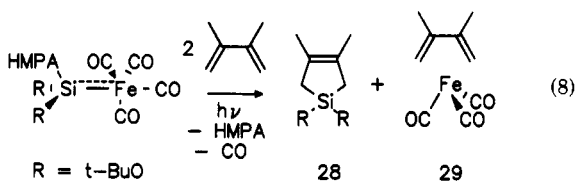

(8)

Silylene complexes have been considered as reactive intermediates particularly in the dehydrogenative coupling of silanes to disilanes with late-transition-metal catalysts. Also, the formation of trisilanes from silanes with Cp_2TiMe_2 and Cp_2ZrMe_2 as catalysts is reported to proceed through silylene complexes.[47] However, in these cases, the Si–Si bond formation reaction occurs in the coordination sphere of the transition metal.

On the other hand, the formation of chain polymers $RH_2Si(RHSi)_nSiH_2R$ from silanes $RSiH_3$ with $Cp^*CpZrSiMe_3H$ as the catalyst appears to proceed by a σ-bond metathesis mechanism.[48]

Base-Free Silylene Complexes as Reactive Intermediates: A Sila-Wittig Reaction

"Base-free" silylene complexes have been identified as reactive intermediates in a variety of silylene transfer reactions. In many cases, the transient (reactive) silylene complexes are also catalytically active species, for instance in silylene transfer reactions to olefins and acetylenes and presumably also in oligomerization reactions of chain polysilanes.[11]

In the series of chromium complexes, the high solubility of $Cr(CO)_5^{2-}$ allows the generation of base-free compounds as reactive intermediates at low temperatures and their derivatization with appropriate trapping reagents.

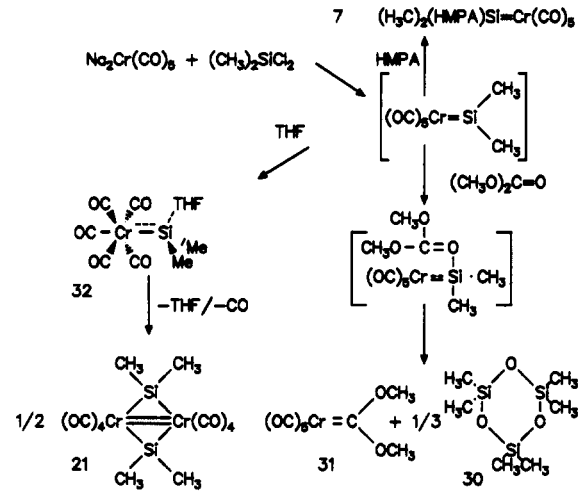

In a solvent-free mixture of $Na_2Cr(CO)_5$, $(H_3C)_2SiCl_2$, and $(MeO)_2CO$, the reactive complex $[(H_3C)_2Si=Cr(CO)_5]$ is generated at −70 °C and trapped by reaction with dimethyl carbonate at ca. −50 °C. As the final reaction products, hexamethyltrisiloxane (**30**) and the (dimethoxycarbene)chromium pentacarbonyl complex **31** (^1H NMR 1.4 ppm) have been isolated. A polar addition complex of dimethyl carbonate and (dimethylsilanediyl)chromium pentacarbonyl has been identified as an intermediate by NMR spectroscopy (^{29}Si NMR 85.0 ppm), which clearly excludes a reaction mechanism in the sense of a concerted [2 + 2] cycloaddition reaction of the silylene complex. Evidence for such a two-step mechanism through a similar polar adduct has recently been provided by Wiberg for the "Wittig reaction" of the silaimine $(t\text{-Bu})_2Si=N-Si(t\text{-Bu})_3$ with benzophenone, $Ph_2C=O$.[49]

In the absence of any trapping reagent, but in the presence of THF, the THF adduct of the chromium complex is obtained, which dimerizes above −40 °C (^{29}Si NMR 159 ppm). The process can be monitored by ^{29}Si NMR spectroscopy. If $Na_2Cr(CO)_5$ and Me_2SiCl_2 are mixed at low temperatures in THF, and HMPA is added subsequently, $Me_2Si=Cr(CO)_5$ is trapped by HMPA to form stable **7** quantitatively.

The reactivity of the Cr=Si double bond with further carbonyl reagents is the subject of current investigations.

"Base-free" silylene complexes have been observed very recently with the complexes $(OC)_4Fe=Si(S\text{-}t\text{-Bu})_2$ (**19**),[50] $[Cp^*Ru(PMe_3)_2=Si(S\text{-}p\text{-Tol})_2^+]BF_4^-$,[51] and $Cp^*_2Si=AuCl$.[13] All compounds are thermolabile and relatively difficult to isolate. The complex $(t\text{-BuS})_2Si=Fe(CO)_4$ could be characterized by spectroscopic methods at low temperatures but decomposes at room temperature to polysilane and iron carbonyl clusters with a half-life of 12 h. However, the compound can be converted into the HMPA adduct **3** by addition of an excess of HMPA. Compound **3** was also characterized by a single-crystal X-ray structure determination.[47] A further base-free complex, $Cp^*Re(CO)_2=Si(t\text{-Bu})_2$, has recently been characterized in our laboratories by spectroscopic methods.

(44) West, R. In *The Chemistry of Organosilicon Compounds*; Patai, S., Rappoport, Z., Eds.; Wiley: New York, 1989.
(45) Treatment of **32** with pyridine yields polysilane and the pyridine complex $pyCr(CO)_5$.
(46) Lee, K. E.; Arif, A. M.; Gladysz, J. A. *Chem. Ber.* **1991**, *121*, 309.
(47) (a) Chang, L. S.; Corey, J. Y. *Organometallics* **1989**, *8*, 1885. (b) Corey, J. Y.; Chang, L. S.; Corey, E. R. *Organometallics* **1987**, *6*, 1595.
(48) Woo, H. G.; Tilley, T. D. *J. Am. Chem. Soc.* **1989**, *111*, 8043–8044.
(49) Wiberg, N.; Schurz, K.; Müller, G.; Riede, J. *Angew. Chem.* **1988**, *100*, 979; *Angew. Chem., Int. Ed. Engl.* **1988**, *27*, 935–936.
(50) Leis, C.; Lachmann, H.; Müller, G.; Zybill, C. *Polyhedron* **1991**, *10*, 1163.
(51) Tilley, T. D. IXth International Symposium on *Organosilicon* Chemistry, Edinburgh, Scotland, July 16–20, 1990; Abstract I27.

This compound appears to be stable at room temperature.[8]

Experimental Section

All experiments have been performed under an atmosphere of dry argon; air-sensitive materials were handled by standard Schlenk techniques. All solvents were dried by distillation from NaK alloy or P_4O_{10}. The residual water content was determined by Karl Fischer titration and was generally below 3.5 ppm.

The preparation of di-*tert*-butoxydichlorosilane, disodium pentacarbonylchromate, and disodium decacarbonylditungstate has been described in the literature;[52] all other chemicals were commercially available.

Spectra. IR spectra were recorded on a Nicolet FT 5DX instrument as KBr pellets, Nujol suspensions, or solutions in 0.1-mm KBr cells. ^1H, ^{13}C, and ^{29}Si NMR spectra were recorded on a JEOL GX 400 spectrometer at 400.01, 53.5, and 36.0 MHz and a JEOL FX 270 instrument at 270.1 MHz. ^{29}Si NMR spectra were partially recorded with DEPT and INEPT pulse programs. ^1H and ^{13}C chemical shifts were measured using the solvent resonances as standard; ^{29}Si chemical shifts were referenced to external Me_4Si in the same solvent.

UV irradiations were performed in a quartz apparatus with a 150-W Hg/high-pressure immersion lamp with a flux of 15 W (254 nm), which corresponds to 0.115 mol equiv/h. The reactions were performed with quantum yields between 1 and 3%.

Mass spectra were measured on a Varian MAT311A instrument by EI ionization at 70 eV or CI or FD techniques by Ms. M. Dumitrescu and Professor F. R. Kreissl.

GC–MS separation was performed on a Hewlett-Packard 5890 A/5970 B instrument equipped with a CP SIL 5CB column.

Cyclic voltammograms were measured under an atmosphere of nitrogen at Pt electrodes with a Ag/AgCl electrode (0.1 M KCl) as reference by Dipl.-Chem. R. Albach.

Microanalyses were done by Mikroanalytisches Laboratorium der Technischen Universität München by Ms. U. Graf and M. Barth.

(*t*-BuO)$_2$(HMPA)Si=Fe(CO)$_4$ (1), (Di-*tert*-butoxysilanediyl)iron(0) Tetracarbonyl–Hexamethylphosphoric Triamide. 1 was prepared by mixing 3.6 g (14.8 mmol) of di-*tert*-butoxydichlorosilane at −40 °C with a suspension of 5.1 g (14.8 mmol) of $Na_2Fe(CO)_4 \cdot 1.5C_4H_8O_2$ ($C_4H_8O_2$ = dioxane) in 50 mL of THF. After addition of 1 mL of HMPA and filtration at −30 °C, the brown solution was transferred onto a cooled (−20 °C) chromatography column. 1 was eluted with THF as the fastest running, almost colorless fraction. The solvent was stripped off under vacuum, and 1 was obtained as a white powder: yield 0.91 g (12%); mp 163 °C. 1 can be crystallized from a saturated THF solution at −15 °C. ^1H NMR ($C_6D_5CD_3$, −48.1 °C): δ 1.60 (s, 18 H, CH_3), 2.20 (d, 18 H, $^3J(^{31}P^1H)$ = 10.4 Hz, *HMPA*). ^{13}C NMR (C_6D_6, 27 °C): δ 31.90, 72.50 (s, *t-Bu*), 36.1 (d, $^2J(^{31}P^{13}C)$ = 26.4 Hz, *HMPA*). IR (cm^{-1}, KBr): 2005 (w), 1920 (vs), 1883 (vs) (ν_{CO}). MS (EI, 70 eV; *m/e* (relative intensity)): 512 (M^+, 0.3%). Anal. Calcd for $C_{18}H_{36}FeN_3O_7PSi$ (M_r 512.4): C, 41.46; H, 6.96; Fe, 10.71; N, 8.06; Si, 5.39. Found: C, 41.37; H, 6.95; Fe, 10.58; N, 8.10; Si, 5.35.

(MesO)$_2$Si(HMPA)=Fe(CO)$_4$ (2), (Dimesitylsilanediyl)iron(0) Tetracarbonyl–Hexamethylphosphoric Triamide. The preparation of 2 was done analogously to the synthesis of 1 from $(MesO)_2SiCl_2$ and $Na_2Fe(CO)_4$. $(MesO)_2SiCl_2$ is available by deprotonation of MesOH with MeLi and subsequent reaction of the obtained MesOLi with $SiCl_4$: yield 31%; mp 155 °C. ^1H NMR: δ 2.13 (s, 6 H, *p*-CH_3), 2.16 (s, 12 H, *o*-CH_3), 2.56 (d, 18 H, *HMPA*, $^3J(^{31}P^1H)$ = 10.2 Hz), 6.65 (s, 4 H, C_6H_2). Anal. Calcd for $C_{29}H_{36}FeN_3O_7PSi$: C, 58.53; H, 6.00. Found: C, 58.07; H, 6.13. MS (EI, 70 eV; *m/e* (relative intensity)): 368 (M^+, 1.4). IR (cm^{-1}, KBr): 1840 (vs), 1860 (vs), 1886 (s), 2012 (w) (ν_{CO}).

Me$_2$(HMPA)Si=Fe(CO)$_4$ (4), (Dimethylsilanediyl)iron(0) Tetracarbonyl–Hexamethylphosphoric Triamide, and Cl$_2$(HMPA)Si=Fe(CO)$_4$ (5), (Dichlorosilanediyl)iron(0) Tetracarbonyl–Hexamethylphosphoric Triamide. 4 and 5 were prepared as described for 1. A 3.1-g (9.1-mmol) amount of $Na_2Fe(CO)_4$ was dissolved in a mixture of 150 mL of THF and 20 mL of HMPA. At −45 °C 1.1 mL (9.1 mmol) of Me_2SiCl_2 was added and the mixture was stirred for a further 3 h at room temperature. Precipitated NaCl was separated by filtration, and the volatile components were removed under high vacuum (10^{-5} bar, 50 °C, 10 h). The viscous residue was dissolved in 20 mL of THF and layered with 20 mL of pentane. The compound crystallizes as colorless cubes.

4: yield 0.63 g (17%); mp 156 °C. ^1H NMR (C_6D_6): δ 0.77 (s, 6 H, H_3CSi), 1.90 (d, 18 H, $^3J(^{31}P^1H)$ = 4.6 Hz, H_3CN). ^{13}C NMR (C_6D_6): δ 11.01 (s, H_3CSi), 26.39 (d, $^3J(^{31}P^{13}C)$ = 4.6 Hz, H_3CN), 218.87 (s, *CO*). ^{29}Si NMR (C_6D_6): δ 92.4 (d, $^2J(^{31}P^{29}Si)$ = 17.5 Hz). MS (*m/e* (relative intensity)): 405 (M^+, 0.9%). Anal. Calcd for $C_{12}H_{24}FeN_3O_5PSi$ (M_r 405.13): C, 35.54; H, 5.92; N, 10.36. Found: C, 35.95; H, 5.15; N, 10.61.

5: yield 38%; mp 123 °C. ^1H NMR (C_6D_6): δ 2.0 (d, 18 H, $^3J(^{31}P^1H)$ = 10.6 Hz, H_3CN). ^{29}Si NMR (C_6D_6): δ 49.7 (d, $^2J(^{31}P^{29}Si)$ = 31.2 Hz). Anal. Calcd for $C_{10}H_{18}Cl_2FeN_3O_5PSi$ (M_r 446.083): C, 26.93; H, 4.07; N, 9.42. Found: C, 26.03; H, 4.01; N, 9.42.

(*t*-BuO)$_2$(HMPA)Si=Cr(CO)$_5$ (6), (Di-*tert*-butoxysilanediyl)chromium(0) Pentacarbonyl–Hexamethylphosphoric Triamide. To a solution of 0.4 g (1.0 mmol) of $Na_2Cr(CO)_5$ in 50 mL of THF was added 1 equiv (0.24 g, 1 mmol) of 3 at −40 °C over a period of 20 min. The yellow mixture was worked up by filtration and column chromatography as described above. The THF adduct was not isolated but transformed into the HMPA adduct 6 by addition of 179 mg (1.0 mmol) of HMPA. 6 crystallizes from a saturated THF solution as colorless rods: yield 0.065 g (12%); mp 144 °C dec. ^1H NMR ($C_6D_5CD_3$, −51 °C): δ 1.60 (s, 18 H, CH_3), 12.30 (d, 18 H, $^3J(^{31}P^1H)$ = 10.6 Hz, *HMPA*). ^{13}C NMR ($C_6D_5CD_3$, −49 °C) δ 36.90, 27.77 (s, *t-Bu*), 32.33 (d, $^2J(^{31}P^{13}C)$ = 5.8 Hz, *HMPA*), 228.1, 224.7 (s, *CO*). ^{29}Si NMR (C_6D_6, 27 °C): δ 12.7 (d, $^2J(^{31}P^{29}Si)$ = 37.2 Hz). IR (cm^{-1}, KBr): 2015 (w), 1991 (vs), 1930 (vs). MS (70 eV, EI; *m/e* (relative intensity)): 545 (M^+, 4.3). Anal. Calcd for $C_{19}H_{36}CrN_3O_8PSi$ (M_r 545.6): C, 41.83; H, 6.65; N, 7.70; Si, 5.15; Cr, 9.53. Found: C, 41.59; H, 6.74; N, 7.95; Si, 5.10; Cr, 9.49.

(CH$_3$)$_2$(HMPA)Si=Cr(CO)$_5$ (7), (Dimethylsilanediyl)chromium(0) Pentacarbonyl–Hexamethylphosphoric Triamide, and Cl$_2$(HMPA)Si=Cr(CO)$_5$ (8), (Dichlorosilanediyl)chromium(0) Pentacarbonyl–Hexamethylphosphoric Triamide. A 2.7-g (11.2-mmol) amount of $Na_2Cr(CO)_5$ was mixed with 1.4 mL (11.2 mmol) of Me_2SiCl_2. The high solubility of $Na_2Cr(CO)_5$ in THF allows the use of only stoichiometric amounts of HMPA. The obtained reaction mixture was worked up as described for 6. The compounds are crystallized from THF in the form of slightly yellow needles.

7: yield 1.1 g (23%); mp 107 °C. ^1H NMR (C_6D_6): δ 0.84 (s, 6 H, H_3CSi), 2.08 (d, 18 H, $^3J(^{31}P^1H)$ = 9.8 Hz, H_3CN). ^{13}C NMR (C_6D_6): δ 11.01 (s, H_3CSi), 36.1 (d, $^2J(^{31}P^{13}C)$ = 5.5 Hz, $(H_3C)_2N$), 211.5 (s, CO_{eq}), 225.53 (s, CO_{ax}). MS (*m/e* (relative intensity)): 429 (M^+, 0.3%). IR (Nujol, cm^{-1}): 2100 (w), 2075 (w), 1975 (s) (ν_{CO}); 900 (ν_{PO}); 580 (ν_{PN}). Anal. Calcd for $C_{13}H_{24}CrN_3O_6PSi$ (M_r 429.28): C, 36.36; H, 5.59; N, 9.79; Cr, 12.12; Si, 6.53. Found: C, 36.39; H, 5.72; N, 9.92; Cr, 12.21; Si, 6.40.

8: ^1H NMR (C_6D_6) δ 2.30 (d, $^3J(^{31}P^1H)$ = 10.7 Hz); ^{29}Si NMR (C_6D_6) δ 55.0 (d, $^2J(^{31}P^{29}Si)$ = 41.4 Hz). Anal. Calcd for $C_{11}H_{18}Cl_2CrN_3O_6PSi$ (M_r 470.242): C, 28.10; H, 3.86; N, 8.84. Found: C, 29.0; H, 4.0; N, 8.34.

(1-AdaO)$_2$(HMPA)Si=Cr(CO)$_5$ (9), (Bis(1-adamantyloxy)silanediyl)chromium(0) Pentacarbonyl–Hexamethylphosphoric Triamide, (2-AdaO)$_2$(HMPA)Si=Cr(CO)$_5$ (10), (Bis(2-adamantyloxy)silanediyl)chromium(0) Pentacarbonyl–Hexamethylphosphoric Triamide, (NepO)$_2$(HMPA)Si=Cr(CO)$_5$ (11), (Bis(neopentyloxy)silanediyl)chromium(0) Pentacarbonyl–Hexamethylphosphoric Triamide, and (TritylO)$_2$(HMPA)Si=Cr(CO)$_5$ (12), (Bis((triphenylmethyl)oxy)silanediyl)chromium(0) Pentacarbonyl–Hexamethylphosphoric Triamide. The oxo compounds 9–12 were prepared by the same procedure described for 1. In all cases the necessary dichlorosilanes were obtained by reaction of $SiCl_4$ with the lithium salts of the respective alcohols.

9 (1-Ada): ^1H NMR (C_6D_6) δ 1.0, 1.34, 1.89 (6:3:6), 2.0; ^{29}Si NMR (C_6D_6) δ 11.9 (d, $^2J(^{31}P^{29}Si)$ = 30.1 Hz). Anal. Calcd for $C_{31}H_{48}CrN_3O_8PSi$ (M_r 701.794): C, 53.06; H, 6.89; N, 5.99. Found: C, 52.61; H, 6.99; N, 6.01.

(52) Brauer, G. *Handbuch* der präparativen *Chemie*; Enke: Stuttgart, FRG, 1984; Vol. 3.

10 (2-Ada): ^{1}H NMR ($CDCl_3$) δ 4.61 (s, 1 H, C1), 1.60 (m br, 2 H, C2), 1.70, 1.86 (d m, $^3J(^1H^1H)$ = 4 Hz, 4 H, C3), 2.40 (dd, $^3J(^1H^1H)$ = 4 Hz, 2 H, C4), 0.90 (d m, $^3J(^1H^1H)$ = 2 Hz, 2 H, C5), 2.10 (d, $^3J(^{31}P^1H)$ = 10 Hz, 18 H, HMPA); ^{29}Si NMR (C_6D_6) δ 11.7 (d, $^2J(^{31}P^{29}Si)$ = 30.2 Hz). Anal. Calcd for $C_{31}H_{48}CrN_3O_8PSi$ (M_r 701.794): C, 53.06; H, 6.89; N, 5.99. Found: C, 53.91; H, 6.95; N, 6.01.

11 (Nep): ^{1}H NMR (C_6D_6) δ 1.08 (s, 18 H, CH_3), 2.21 (d, $^3J(^{31}P^1H)$ = 10.2 Hz, 18 H, *HMPA*), 3.70, 3.80 (AB system, gem $^2J(^1H^1H)$ = 9.8 Hz, 4 H, CH_2 (prochiral)); ^{13}C NMR (C_6D_6) δ 26.9 (s, CH_3), 33.1 (s, $C(CH_3)_3$), 36.34 (d, $^2J(^{31}P^{13}C)$ = 5.5 Hz, *HMPA*), 72.64 (s, CH_2), 223.78 (s, *CO*). Anal. Calcd for $C_{21}H_{40}CrN_3O_8PSi$ (M_r 573.620): C, 43.97; H, 7.03; N, 7.33. Found: C, 44.51; H, 7.12; N, 7.38.

12 (trityl): ^{1}H NMR (C_6D_6) δ 7.3 (br, 30 H, C_6H_5), 2.01 (d, $^3J(^{31}P^1H)$ = 11.0 Hz, 18 H, H_3CN); ^{29}Si NMR (C_6D_6) δ 10.9 (d, $^2J(^{31}P^{29}Si)$ = 32.0 Hz). Anal. Calcd for $C_{49}H_{48}CrN_3O_8PSi$ (M_r 917.992): C, 64.11; H, 5.27; N, 4.58. Found: C, 65.10; H, 5.31; N, 4.61.

(*t*-BuO)$_2$(HMPA)Si=W(CO)$_5$ (13), (Di-*tert*-butoxysilanediyl)tungsten(0) Pentacarbonyl-Hexamethylphosphoric Triamide. 13 has been synthesized from $Na_2W_2(CO)_{10}$ and $(t\text{-BuO})_2SiCl_2$ analogously to the method for 6: yield 73%. ^{1}H NMR (C_6D_6): δ 1.65 (s, 18 H, *t-Bu*), 2.10 (d, $^3J(^{31}P^1H)$ = 10.1 Hz, *HMPA*). ^{13}C NMR ($C_6D_5CD_3$, 22 °C): δ 35.90, 28.10 (s, *t-Bu*), 33.11 (d, $^2J(^{31}P^{13}C)$ = 11.0 Hz, *HMPA*), 229.1, 223.4 (s, *CO*). Anal. Calcd for $C_{19}H_{36}N_3O_8PSiW$ (M_r 677.420): C, 33.69; H, 5.36; N, 6.20. Found: C, 32.90; H, 5.34; N, 6.25.

X-ray Structure Determination of 4, 5, 7, and 8. Suitable single crystals of 4, 5, 7, and 8 were grown from solution (in all cases THF layered with pentane). The crystals were sealed into glass capillaries under argon at dry ice temperature. A summary of the crystal data and important numbers pertinent to data collection and structure refinement is given in Table VI.

Diffractometer measurements showed the Fe complexes 4 and 5 and the Cr complexes 7 and 8, respectively, to be isostructural, which was confirmed by structure refinement. Exact cell dimensions were obtained by least-squares refinement on the Bragg angles of 15 selected reflections centered on the diffractometer. Reduced cell calculations did not indicate cell symmetry higher than monoclinic for all four compounds. The integrated intensities were collected on a Syntex $P2_1$ diffractometer with graphite-monochromated Mo Kα radiation (λ = 0.710 69 Å, scan speed (in θ) 0.7–29.3°/min). Repeated measurement of three standard reflections did not indicate significant crystal decay or misalignment during the data collection. The intensity data were corrected for Lp effects and those of 5, 7, and 8 also for absorption. For the latter correction scans at 10° intervals around the diffraction vectors of 7 reflections (8: 11 reflections) near χ = 90° served to evaluate the relative transmissions. The structure of 5 was solved by direct methods and completed by Fourier techniques. The refined positions of the non-H atoms of 5 served as a starting point for the refinement of 4. Likewise, the solved structure of 7 (Patterson techniques) could be used for the refinement of 8. The non-H atoms of all four structures were refined with anisotropic displacement parameters in one large block. For 4 and 5, the H atom positions were held constant during refinement (U_{iso} = 0.05 Å^2); for 7 and 8 the methyl groups were refined as rigid groups. In the refinement of 4, three structure factors were suppressed which apparently had resulted from faulty intensity measurements; for 7, one structure factor was suppressed.

Atomic form factors for neutral, isolated atoms were those of Cromer and Waber;[53] those for hydrogen were based on the bonded, spherical model of Stewart, Davidson, and Simpson.[54] Corrections for anomalous scattering were applied for all atoms except hydrogen.[55] The programs used included SHELXS-86[56] (structure solution), SHELX-76[57] (refinement), and ORTEP[58] (molecular drawings), as well as locally written routines. Tables VII–X contain the atomic coordinates and equivalent isotropic displacement parameters; Figures 1–4 show the molecular structures and the crystallographic numbering scheme adopted. Further data for the structure determinations are available as supplementary material.

MO Calculations for the Silylenes Si(OMe)$_2$, SiMe$_2$, and SiCl$_2$. The calculations have been done with a semiempirical MNDO method with the program QCPE017. The SCF iterations converged to the final results after 15–30 cycles. For details see ref 62.

Molecular Modeling of the Structures of 1 and 4–8. The molecules were optimized by the ALCHEMY minimizer program with $E_{tot} = E_{str} + E_{ang} + E_{tor} + E_{vdw}$: E_{tot} = total energy; $E_{str} = \sum_{i=1}^{N} k^d_i/2(d_i - d^0_i)^2$, d^0_{FeSi} = 2.300 Å, $d_{\theta(CrSi)}$ = 2.400 Å, k_{FeSi} = 1500 kcal/(mol Å^2), k_{CrSi} = 1500 kcal/(mol Å^2); $E_{ang} = \sum_{i=1}^{N} k^\theta_i/2(\theta_i - \theta^0_i)^2$, θ^0_{FeSiO} = 115°, k^θ_{FeSiO} = 0.03 kcal/(mol deg^2), θ^0_{CrSiO} = 115°, k^θ_{CrSiO} = 0.03 kcal/(mol deg^2); $E_{tor} = \sum_{i=1}^{N} k_i/2(1 + (\sin \mathrm{per}_i)\cdot[\cos(|\mathrm{per}_i|\omega_i)])$, $\omega_{SiFe^{**}}$ = 0.1 kcal/(mol deg^2), $\omega_{SiCr^{**}}$ = 0.1 kcal/(mol deg^2); $E_{vdw} = \sum_{i=1}^{N}(\sum_{j>i} E_{ij}[1.0/a^{12}_{ij} - 2.0/a^6_{ij}])$, E_{FeSi} = 0.200 kcal/mol, E_{CrSi} = 0.200 kcal/mol, R_{Fe} = 3.000 Å, R_{Cr} = 3100 Å, R_{Si} = 2.000 Å. All other parameters were used from the program without modification.

Photolytic Generation of the Complexes *trans*-(Di-*tert*-butoxysilanediyl)(triphenylphosphine)iron(0) Tetracarbonyl-Hexamethylphosphoric Triamide (23) and *trans*-(Dimethylsilanediyl)(triphenylphosphine)iron(0) Tetracarbonyl-Hexamethylphosphoric Triamide (24) from 1 and 4. The photolysis reaction of 1 or 4 was carried out at −40 °C in a quartz apparatus equipped with a 150-W Hg high-pressure immersion lamp.

A solution of 1.54 g (3 mmol) of 1 or 1.22 g (3 mmol) of 4, respectively, and 787 mg (3 mmol) of $(C_6H_5)_3P$ in 100 mL of THF was photolyzed at −40 °C for 12 h. The initially colorless solution rapidly turned to orange. Without irradiation, no reaction was observed at 20 °C within a period of 24 h.

After removal of all volatile components, the *trans*-phosphine/silylene complexes 23 and 24 were isolated as orange powders. Compounds 23 and 24 can also be crystallized from THF as orange needles.

23: yield 1.52 g (79%). ^{1}H NMR (C_6D_6, 22 °C): δ 1.7 (s, 18 H, *t*-BuO), 2.5 (d, $^3J(^{31}P^1H)$ = 10.5 Hz, 18 H, HMPA), 7.0–7.3 (br, 15 H, C_6H_5). ^{31}P NMR (C_6D_6, 23 °C): δ 87.8. IR (KBR): 1961 (vs). Anal. Calcd for $C_{35}H_{51}FeN_3P_2O_6$ (M_r 755.689): C, 55.63; H, 6.80; N, 5.56; P, 8.20. Found: C, 54.91; H, 6.88; N, 5.60; P, 8.11.

24: yield 1.70 g (75%). ^{1}H NMR (C_6D_6, 22 °C): δ 0.7 (d, 6 H, H_3CSi), 2.5 (d, $^3J(^{31}P^1H)$ = 10.5 Hz, H_3CN), 7.0–7.3 (br, 15 H, C_6H_5). IR (KBr): 1861 (vs). Anal. Calcd for $C_{29}H_{39}FeN_3O_4P_2Si$ (M_r 639.529): C, 54.46; H, 6.15; N, 6.57; P, 9.69. Found: C, 53.90; H, 6.20; N, 6.57; P, 9.71.

***trans*-[(C$_6$H$_5$)$_3$P]$_2$Fe(CO)$_4$ (25), *trans*-Bis(triphenylphosphine)iron(0) Tricarbonyl.** Further irradiation of 2.27 g (3 mmol) of 23 or 1.92 g (3 mmol) of 24, respectively, in the presence of 787 mg (3 mmol) of $(C_6H_5)_3P$ at 21 °C for 12 h yielded an intensely red solution. After removal of the solvents, 25 was isolated either by direct crystallization from a saturated (ca. 10 mL) THF solution of the crude product mixture or after purification by column chromatography (silica gel, 30-cm length, 1.5-cm diameter, water-cooled jacket, elution with THF as fastest running red zone): yield 1.73 g (86.7%) of 25; red microcrystalline material. The polysilanes were isolated by chromatography over Florisil (Mg silicate, separation of 25). Prolonged extraction of the Florisil (after chromatographic separation of 25) with approximately 600 mL of THF (colorless fraction) yields, after evaporation of the volatile components, 154 mg of $[(t\text{-BuO})_2Si]_n$ (viscous oil) or 121 mg of $(Me_2Si)_n$ (beige powder).

25: ^{1}H NMR (C_6D_6) δ 7.1 (m, 18 H), 7.5–8.0 (m, 12 H); ^{31}P NMR (C_6D_6) δ 95.2; IR (cm^{-1}, KBr) 1985 (vs). Anal. Calcd for $C_{39}H_{30}FeO_3P_2$ (M_r 664.461): C, 70.50; H, 4.55; P, 9.32. Found: C, 69.80; H, 4.51; P, 9.10.

(53) Cromer, D. T.; Waber, J. T. *Acta Crystallogr.* **1965**, *18*, 104.
(54) Stewart, R. F.; Davidson, E. R.; Simpson, W. T. *J. Chem. Phys.* **1965**, *42*, 3175.
(55) *International Tables for X-ray Crystallography*; Kynoch Press: Birmingham, England, 1974; Vol. IV (present distributor: Kluwer Academic Publishers, Dordrecht, The Netherlands).
(56) Sheldrick, G. M. In *Crystallographic Computing 3*; Sheldrick, G. M., Krüger, C., Goddard, R., Eds.; Oxford University Press: Oxford, England, 1985; p 175.
(57) Sheldrick, G. M. SHELX-76, Program for Crystal Structure Determination; University of Cambridge: Cambridge, England, 1976.
(58) Johnson, C. K. ORTEP-II; Report ORNL-5138; Oak Ridge National Laboratory: Oak Ridge, TN, 1976.

Table XIV. Kinetic Data for the Photolytic Generation of 23 ($[(C_6H_5)_3P]$ = 10.0 mmol L^{-1})

	yield/10^3 mol L^{-1}			yield/10^3 mol L^{-1}	
time/10^{-3} s	1	23	time/10^{-3} s	1	23
0.6	9.486	0.514	72	6.061	3.939
12	9.023	0.977	108	5.064	4.936
18	8.604	1.396	144	4.349	5.651
24	8.220	1.450	180	3.810	6.190
30	7.869	2.131	216	3.391	6.609
36	7.549	2.452	432	2.041	7.959

$(Me_2Si)_n$: ^1H NMR (C_6D_6, 22 °C) δ 0.2 (s, br, CH_3); ^{29}Si NMR δ −22.1; IR (Nujol) no bands for ν_{SiO} vibration; mass spectrum (EI, 70 eV) highest observable mass m/e 752, typical Gaussian peak distribution in intervals of m/e 58 ($-Me_2Si$) with basis peak at m/e 57. A cryoscopic molecular weight determination of $[Me_2Si]_n$ in dioxane gave M_n = 550 (±50).

$[(t\text{-BuO})_2Si]_n$: ^1H NMR (C_6D_6, 22 °C) δ 1.2 (s, br, *t*-BuO); ^{29}Si NMR δ −71.2.

***trans*-(Di-*tert*-butoxysilanediyl)(triphenylphosphine)-chromium(0) Tetracarbonyl–Hexamethylphosphoric Triamide (26).** A solution of 1.64 g (3.0 mmol) of **6** and 787 mg (3 mmol) of $(C_6H_5)_3P$ in 100 mL of THF was irradiated for 12 h at −40 °C. The reaction mixture turned red upon photolysis. Without irradiation, no reaction occurred at 22 °C over a period of 24 h. After evaporation of the solvent under high vacuum, **26** was isolated as a red microcrystalline material: yield 1.75 g (75%). ^1H NMR (C_6D_6): δ 1.7 (d, 6 H, *t*-BuO), 2.5 (d, $^3J(^{31}P^1H)$ = 10.5 Hz, H_3CN), 7.0–7.3 (m, 15 H, C_6H_5). ^{31}P NMR (C_6D_6): δ 87.8. IR (cm^{-1}, KBr): 1860 (vs). Anal. Calcd for $C_{36}H_{51}CrN_3O_7P_2Si$ (M_r 779.848): C, 55.45; H, 6.59; N, 5.39; P, 7.94. Found: C, 56.10; H, 6.61; N, 5.39; P, 7.80.

***trans*-$[(C_6H_5)_3P_2]Cr(CO)_4$ (27), *trans*-Bis(triphenylphosphine)chromium(0) Tetracarbonyl.** Irradiation of the orange solution of 1.56 g (2.0 mmol) of **26** and 525 mg (2.0 mmol) of $(C_6H_5)_3P$ gave after 12 h at 15 °C a dark red solution. Evaporation of the solvents under high vacuum yielded 1.31 g (95% yield) of **27** as a brown-red powder. The polysilane could also be isolated as described above by extraction from a Florisil column with THF. ^1H NMR (C_6D_6): δ 7.1 (m, 18 H), 7.5–8.0 (m, 12 H). ^{31}P NMR (C_6D_6): δ 79.6. IR (cm^{-1}, KBr): 1958 (vs). Anal. Calcd for $C_{40}H_{30}CrO_4P_2$ (M_r 688.620): C, 69.77; H, 4.39; P, 9.00. Found: C, 69.70; H, 4.40; P, 8.89.

Kinetic Investigations of the Photolysis of 1 in the Presence of $(C_6H_5)_3P$. A solution of 512.0 mg (10 mmol L^{-1}) of **1** in 100.0 mL of THF was photolyzed at −40.0 °C in the presence of 262.3 mg (10 mmol L^{-1}) of $(C_6H_5)_3P$. Aliquots of 0.1 mL were taken (syringe) every 600 s, and the quantitative evaluation of the compounds was done by both IR and ^1H NMR spectroscopy. The components **1** and **23** were identified by their typical ν_{CO} frequencies at 2005/1920 (**1**) and 1961 cm^{-1} (**23**); the measurement of the concentrations was done by integration of the IR bands or the ^1H NMR lines, respectively. The temperature of the reaction mixture was equilibrated and maintained with ±1 °C.

Analysis of the data led to the rate law $-dC_{23}/dt = k[(C_6H_5)_3P][1]$, with $k = 8.918 \times 10^{-3}$ L mol^{-1} s^{-1}. The quantum yield for the reaction (254-nm line) was Φ = 0.021. Equal concentrations of the reactants ([phosphine] = [1]) allowed an integration of the rate law to give $1/C_t - 1/C_0 = kt$, which was fulfilled by the experimental data with the regression coefficient r = 0.9991.

The time dependence for the formation of **23** was found as shown in Table XIV. With a phosphine concentration of 524.6 mg (20.0 mmol L^{-1}) and 512.0 mg (10.0 mmol L^{-1}) of **1**, the time dependence shown in Table XV was observed (−40.0 °C). In this case, the linear regression analysis gave $k = 5.819 \times 10^{-3}$ L mol^{-1} s^{-1} with a regression coefficient r = 0.982. Identical values were observed for $C_{phosphine}$ = 262.3 mg (10 mmol L^{-1}) and C_1 = 1.024 g (20 mmol L^{-1}) at −40 °C. For further experimental details see also ref 12.

Photolysis of 1 in the Presence of 2,3-Dimethylbutadiene. A 1.54-g (3-mmol) amount of **1** in 100 mL of THF was photolyzed at −40 °C in the presence of 5.0 g of 2,3-dimethylbutadiene for 12 h. The mixture was purified by column chromatography over silica gel with THF as eluent; detection of the fractions was done with a long-wave UV lamp. The first fraction contained the silacyclopentane **28**; as the second fraction, the 2,3-dimethylbutadiene complex **29** was observed. Furthermore, a GC–MS analysis of the crude reaction products shows, besides solvent peaks, two major peaks at retention time 6.2 min, 70% intensity, m/e 256, M^+ for **28** and retention time 5.2 min, 20% intensity, m/e 222, M^+ for **29** as well as traces (0.9%) of HMPA, M^+ at m/e 179.

Table XV. Kinetic Data for the Photolysis Reaction of 1 for the Phosphine Concentration $[(C_6H_5)_3P]$ = 20.0 mmol L^{-1}

$t/10^3$ s	$C_{phosphine}/10^3$ mol L^{-1}	$C_{23}/10^3$ mol L^{-1}	$C_1/10^3$ mol L^{-1}
3.6	17.55	7.55	2.452
7.2	16.06	6.06	3.939
10.8	15.06	5.06	4.936

28: ^1H NMR (C_6D_6) δ 1.74 (br, 10 H, CH_3, CH_2), 1.70 (s, 18 H, *t*-BuO); MS (EI, 70 eV; m/e) 256.[59]

29: ^1H NMR (C_6D_6) δ 6.30, 5.92 (AB system, $^2J(^1H^1H)$ = 21 Hz, 4 H, CH_2), 1.65 (s, 6 H, CH_3): IR (KBr; cm^{-1}) 2045 (s), 1971 (s) (ν_{CO}). Anal. Calcd for $C_9H_{10}FeO_3$ (M_r 222.023): C, 48.69; H, 4.54. Found: C, 47.80; H, 4.55.[60]

Thermolysis of 4. A 1.12-g (2.19-mmol) amount of **4** dissolved in 50 mL of THF was refluxed for 21 h. The resulting mixture was subjected to chromatography on Florisil (column of 2-cm diameter and ~30-cm height). The first fraction (detection with long-wave UV lamp), containing unreacted **4**, was dismissed and the polysilane extracted from the column by prolonged eluation with THF. After evaporation of the solvent, 46 mg of $[Me_2Si]_n$ was isolated. Identification was done by NMR and IR spectroscopy.

Alternatively, 522 mg (1.02 mmol) of **4** was heated to 115 °C for 20 min under a vacuum of 10^{-4} Torr. Above the melting point of **4**, HMPA distilled off (and can be trapped at a cooling finger) and **22** was formed. **22** was crystallized from THF; yield 153 mg (33.8%). ^1H NMR (C_6D_6, 22 °C): δ 0.51 (s). ^{29}Si NMR (C_6D_6): δ 161.0 (s). Mass spectrum (EI, 70 eV; m/e): 452 (0.5%, M^+). Anal. Calcd for $C_{12}H_{12}Fe_2O_8Si_2$ (M_r 452.086): C, 31.88; H, 2.68. Found: C, 30.91; H, 2.70.

Further heating of **22** for several hours at 155 °C led to the decay of the compound with formation of iron carbonyl clusters. Small amounts (ca. 3 mg) of $Fe_3(CO)_{12}$ could be sublimed onto a cooling finger (IR (hexane) 2046, 2023 cm^{-1}). Extended chromatography of the reaction mixture on Florisil yielded traces (ca. 3 mg) of poly(dimethylsilane). The dark iron-containing (83% Fe) residue exhibited weak IR bands at 2041/2020 cm^{-1} but did not migrate significantly upon chromatography.

Reaction of $[Me_2Si{=}Cr(CO)_5]$ with DMC. A 0.7-g (3.2-mmol) amount of $Na_2Cr(CO)_5$ was mixed with 0.38 mL (3.3 mmol) of Me_2SiCl_2 at −60 °C and 5 mL of dimethyl carbonate was added. The mixture was thawed slowly and finally warmed to room temperature over a period of 1 h. The color of the mixture changed from orange to red and again to orange during this process. A sample of a freshly prepared reaction mixture gives a ^{29}Si NMR shift of 85.0 ppm at −45 °C for $Me_2Si(DMC){=}Cr(CO)_5$ (^1H NMR (toluene-d_8) δ 0.82 (s, 6 H, H_3CSi), 1.38 (s, 6 H, H_3CO)). The peaks disappeared above −30 °C, and new NMR signals were observed (^{29}Si NMR δ −9.9; ^1H NMR δ 0.31) indicating the formation of $(Me_2SiO)_3$.[61] GC–MS analysis of the crude reaction products at room temperature gave, besides solvent peaks, a peak with retention time 1.7 min and the molecular mass of an authentic sample of $(Me_2SiO)_3$. After filtration and removal of the volatile components, crude **31** was isolated as a yellow oil.

31 was further purified by column chromatography over silica gel (50-cm height, 1.5-cm diameter, −30 °C); yield 102.2 mg (12%). ^1H NMR (C_6D_6): δ 1.4 (s, H_3CO). ^{13}C NMR: 34.0 (CH_3), 204.3

(59) For comparison see: Ishikawa, M.; Ohi, F.; Kumada, M. *J. Organomet. Chem.* **1975**, *86*, C23.

(60) Fischer, E. O.; Werner, H. *Metal π-Complexes 1*; Elsevier: Amsterdam, 1966.

(61) Horn, H. G.; Marsmann, H. C. *Makromol. Chem.* **1972**, *162*, 255.

(62) Dewar, M. S.; Zoebisch, E. G.; Healy, E. F.; Stewart. J. P. *J. Am. Chem. Soc.* **1985**, *107*, 3902.

(cis CO), 206.5 (trans CO), 290.9 (Cr=C). IR (cm^{-1}): 2015 (w), 1945 (s), 1905 (s) (ν_{CO}). Anal. Calcd for $C_8H_6CrO_7$ (M_r 266.125): C, 36.11; H, 2.27; Cr, 19.54. Found: C, 37.01; H, 2.27; Cr, 19.41.

A mixture of Me_2SiCl_2 and $Na_2Cr(CO)_5$ in THF at −60 °C gave **32**. ^1H NMR (toluene-d_8): δ 0.5 (s, H_3CSi), 1.4, 3.6 (m, *THF*). ^{29}Si NMR (toluene-d_8): δ 97.4. The complex dimerized at room temperature to give **21**. The reaction could also be monitored by ^{29}Si NMR spectroscopy.

21: ^1H NMR (C_6D_6) δ 0.99 (s, H_3C); ^{29}Si NMR (C_6D_6) δ 159.0; MS (EI, 70 eV; *m/e*) 444 (0.5%, M^+), 416 (3%, $M^+ - CO$), further fragments for loss of CO. Anal. Calcd for $C_{12}H_{12}CrO_8Si_2$ (M_r 444.384): C, 32.43; H, 2.72; Cr, 23.40. Found: C, 32.01; H, 2.69; Cr, 22.91.

Acknowledgment. This work was supported by Deutsche Forschungsgemeinschaft, Fonds der Chemischen Industrie, and Bund der Freunde der Technischen Universität München. The Mössbauer spectra were measured at the Physics Department, Technische Universität München, in the laboratories of Professor F. Wagner; cyclic voltammetric measurements were done at the Anorganisch-chemisches Institut by Dipl.-Chem. R. Albach. Dr. M. Heiss provided us with an introduction into the MOPAC program. D.L.W. thanks the Alexander von Humboldt Foundation for a postdoctoral fellowship in 1988–1989. Furthermore, we are indebted to Professor H. Schmidbaur for his continued interest in our investigations.

Supplementary Material Available: Tables of hydrogen atom coordinates and anisotropic displacement parameters for **4**, **5**, **7**, and **8** (16 pages); listings of structure factors (89 pages). Ordering information is given on any current masthead page.

Syntheses, Structures, and Isomerization Processes of Dialkylaluminum Silylamido Complexes

Deborah M. Choquette,† Mary Jo Timm,† Jason L. Hobbs,† M. Marufur Rahim,‡ Kazi J. Ahmed,‡ and Roy P. Planalp*,†

Departments of Chemistry, University of New Hampshire, Durham, New Hampshire 03824, and University of Vermont, Burlington, Vermont 05405

Received May 8, 1991

Reactions of R_3SiNH_2 with R'_3Al in refluxing hexane afford a family of dimeric aluminum silylamides, $[R'_2AlN(H)SiR_3]_2$ (R′ = Me, R_3 = Ph_3, Et_3; R′ = *i*-Bu, R_3 = Ph_3, R_3 = *t*-Bu_2H). $[Me_2AlN(H)SiMe_3]_2$ is prepared from $[Cl_2AlN(H)SiMe_3]_2$ and dimethylmagnesium. X-ray crystallography of $[Me_2AlN(H)SiEt_3]_2$ and $[Me_2AlN(H)SiPh_3]_2$ indicates planar Al_2N_2 ring frameworks with the silyl groups oriented trans about the ring. A distorted-tetrahedral geometry at nitrogen places the silyl groups nearly in the plane of the Al_2N_2 ring, while the N–H bond vector is nearly orthogonal to the Al_2N_2 plane. The degree of distortion depends on the steric bulk of SiR_3. All dimers undergo a cis–trans isomerization process in benzene. This process is fast for methylaluminum compounds but slow for isobutylaluminum ones: the methylaluminum amides attain equilibrium solution isomer distributions of ca. 50/50, while the isobutyl compounds are strongly biased toward the cis or trans isomer and do not attain equilibrium. Isomerization of the methylaluminum compounds is catalyzed by less than one equiv of 4-methylpyridine, while hindered pyridines have no effect. Greater amounts of 4-methylpyridine lead to adduct formation; the adduct $(i\text{-Bu})_2$(4-Me-py)$AlN(H)SiPh_3$ is isolated. A mechanism with rate-determining attack of base at aluminum is discussed. Crystal data for $[Me_2AlN(H)SiPh_3]_2$: M_r = 662.96, triclinic, $P\bar{1}$, a = 8.821 (2) Å, b = 9.435 (3) Å, c = 13.342 (4) Å, α = 70.97 (3)°, β = 74.23 (2)°, γ = 66.02 (2)°, Z = 1, R = 0.041, R_w = 0.042. Crystal data for $[Me_2AlN(H)SiEt_3]_2$: M_r = 374.6, monoclinic, $P2_1/n$, a = 7.095 (3) Å, b = 11.452 (5) Å, c = 15.467 (5) Å, β = 96.83 (3)°, Z = 2, R = 0.055, R_w = 0.052.

Introduction

The well-known reaction of alkylamines with alkylaluminum compounds affords oligomeric or polymeric ring and cage structure aluminum amides and imides.[1] Very few alkylaluminum silylamides have been prepared, however.[2] The possible influence of silyl groups on the geometry and coordinating ability of nitrogen, and therefore the ability of silylamides to function as bridging ligands, is of fundamental interest.[3] Thus, while no monomer of the type $R_2Al–N(R')(R'')$ (R, R′, R″ = alkyl) is presently known, we are interested in preparation of such a monomer (where R′ or R″ = alkylsilyl group), which may exist because of a reduced tendency of nitrogen to form a dimer by bridging aluminum centers. There may be a π interaction between nitrogen and aluminum in such compounds.[4] Known amido monomers, such as $Al[N(SiMe_3)_2]_3$,[5] $Al(N\text{-}i\text{-}Pr_2)_3$,[6] and $(Me_2N)_2AlCl$,[6] have more than one π-donating ligand. Another goal is preparation

† University of New Hampshire.
‡ University of Vermont.

(1) (a) Wiberg, E. In *FIAT Review of German Science 1939–1946*; Bähr, G., Ed.; Dieterische Verlagsbuchhandlung: Wiesbaden, BRD, 1948; Inorganic Chemistry, Part II. (b) Davidson, N.; Brown, H. C. *J. Am. Chem. Soc.* **1942**, *64*, 316. (c) Mole, T.; Jeffery, E. A. *Organoaluminum Chemistry*; Elsevier: New York, 1972. (d) Lappert, M.; Power, P.; Sanger, A.; Srivastava, R. *Metal and Metalloid Amides*; Ellis Horwood: Chichester, U.K., 1980. (e) Jones, J. I.; McDonald, W. S. *Proc. Chem. Soc., London* **1962**, 366. (f) Laubengayer, A. W.; Smith, J. D.; Ehrlich, G. G. *J. Am. Chem. Soc.* **1961**, *83*, 542. (g) McLaughlin, G. M.; Sim, G. A.; Smith, J. D. *J. Chem. Soc., Dalton Trans.* **1972**, 2197. (h) Amirkhalili, S.; Hitchcock, P. B.; Smith, J. D. *J. Chem. Soc., Dalton Trans.* **1979**, 1206. (i) Cesari, M.; Cucinella, S. In *The Chemistry of Inorganic Homo- and Heterocycles*; Haiduc, I., Sowerby, D., Eds.; Academic Press: London, 1987.

(2) (a) Sonnek, G.; Päch, M.; Bredereck, H.; Oswald, L. *J. Organomet. Chem.* **1987**, *329*, 31. (b) Sonnek, G.; Päch, M. *J. Prakt. Chem.* **1987**, *329*, 907. (c) Wiberg, N.; Baumeister, W.; Zahn, P. *J. Organomet. Chem.* **1972**, *36*, 267.

(3) (a) Bartlett, R. A.; Power, P. P. *J. Am. Chem. Soc.* **1987**, *109*, 6509. (b) Cotton, F. A.; Wilkinson, G. *Advanced Inorganic Chemistry*; Wiley: New York, 1988; p 368.

0276-7333/92/2311-0529$03.00/0